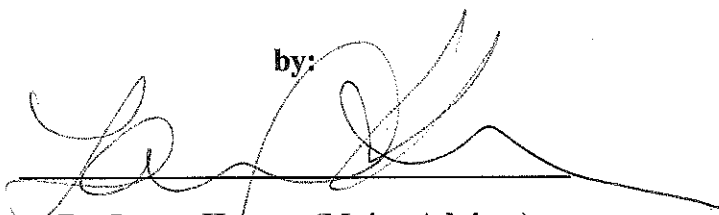
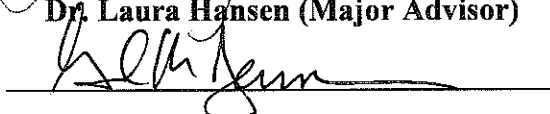


**Thesis Approved**

by:

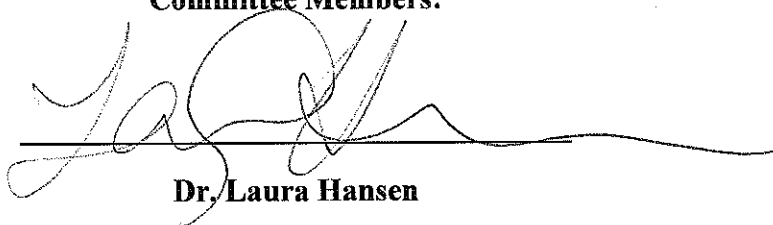
A large, stylized handwritten signature in black ink, appearing to be 'Laura Hansen', written over a horizontal line.

**Dr. Laura Hansen (Major Advisor)**

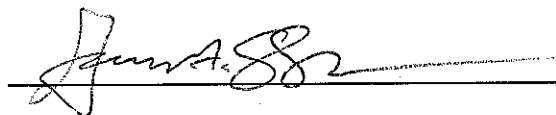
A smaller, more compact handwritten signature in black ink, written over a horizontal line.

**Dean**

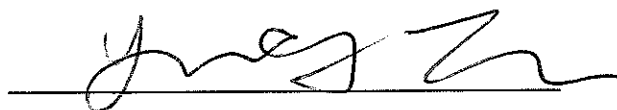
**Committee Members:**

A large, stylized handwritten signature in black ink, appearing to be 'Laura Hansen', written over a horizontal line.

**Dr. Laura Hansen**

A handwritten signature in black ink, appearing to be 'Garrett Soukup', written over a horizontal line.

**Dr. Garrett Soukup**

A handwritten signature in black ink, appearing to be 'Yaping Tu', written over a horizontal line.

**Dr. Yaping Tu**

A handwritten signature in black ink, appearing to be 'Zhaoyi Wang', written over a horizontal line.

**Dr. Zhaoyi Wang**



**The Role of CDC25A in Ultraviolet-induced  
Nonmelanoma Skin Tumorigenesis**

By

Jodi Keiko Hirata Yanagida

**A THESIS**

Submitted to the faculty of the Graduate School of the Creighton University  
in Partial Fulfillment of the Requirements for the degree of  
Master of Science in the Department of Biomedical Sciences

Omaha, NE

October 2010



## The Role of CDC25A in Ultraviolet-Induced Nonmelanoma Skin Tumorigenesis

### Abstract

Cell division cycle 25A (CDC25A) is a dual-specificity phosphatase that removes inhibitory phosphate groups from cyclin-dependent kinases, allowing cell cycle progression. Activation of cell cycle checkpoints following DNA damage can result in degradation of CDC25A, leading to cell cycle arrest. Consistent with its role in cell cycle regulation, CDC25A is over-expressed in multiple types of human cancer. Ultraviolet (UV) irradiation, which causes most skin cancer, results in both DNA damage and CDC25A degradation. In order to investigate the role of CDC25A in the skin's response to UV, we conditionally ablated *Cdc25a* in the skin by crossing *Cdc25a<sup>fl/fl</sup>* mice with transgenic *Krt14* promoter-driven *Cre recombinase* mice. We hypothesized that ablation of CDC25A in the skin would increase cell cycle arrest following UV irradiation, allowing for improved repair of DNA damage and decreasing tumorigenesis. UV-induced DNA damage, in the form of cyclopurine dimers and 8-oxo-deoxyguanosine adducts was eliminated earlier in the *Cdc25a* mutant skin when compared to the UV-exposed controls. Surprisingly, no significant difference in cell cycle regulation after UV exposure was detected in the mutants compared to controls. However, apoptosis was increased in the *Cdc25a* mutants compared to controls 18 hours following UV exposure. Deletion of *Cdc25a* resulted in increased epidermal hyperplasia compared to controls at 36 h post-UV. Although there was no difference in tumor multiplicity, UV-induced papillomas in Tg.AC<sup>+</sup>/*Cdc25a* mutants were significantly smaller than in controls in the first 6 weeks following UV exposure. These data suggest that loss of CDC25A facilitates the rapid repair of DNA damage through increased apoptosis of damaged cells following

exposure to UV, but has surprisingly little effect on cell cycle regulation. Interestingly, improved repair of DNA damage did not result in decreased tumorigenesis. The number of tumors was similar in *Cdc25a* mutant and control mice, although tumors were smaller in the mutants. Thus, in this model, deletion of *Cdc25a* improved the repair of DNA damage and increased apoptosis following UV, but did not substantially alter cell cycle regulation. The cumulative effects of CDC25A deletion in UV-exposed skin did not alter tumor multiplicity in a *v-ras<sup>Ha</sup>* transgenic model but did result in smaller tumors.

## **Dedication**

This thesis is dedicated to my parents who have shown me the importance of working hard and appreciating what I have. Without their encouragement, sacrifices, and unconditional love I would not have gotten to where I am today both in life and in my education. I am truly blessed to have parents who have been by my side every step of the way and have taught me what the most important things in life are. I want to especially thank my mom for all of the invaluable advice and my dad for always making me laugh.

This thesis is also dedicated to my friends at home in Hawaii who have supported me and made me smile when things have not been easy. They gave me the strength to challenge myself in ways I never thought possible. I am so grateful to have them in my life.

## **Acknowledgements**

First of all, thank you to Dr. Hansen for her invaluable guidance, inspiration, and support in completing this research. I'd also like to thank the members of the Hansen Lab who have been integral in allowing me to complete this research through their endless support: Jodi Nicolai, Kyle Bichsel, Yawah Nicholson, Fiona Denge, Abigail Brockhouse, Dr. Velidi Rao, David Lynch, Jenan Al-Matouq, Brianna Hammiller, Michaela Behrens, Amrit Kandel, Tara Fordyce, Patrick Carroll, Jessica Gaulter, Eric Forney, Tim Malouff, David Deertz and Nitin Marwaha.

Thank you to Dr. Susan Repertinger for histopathological characterization of my tumor and skin samples. Thanks also to Dr. Greg Perry for running our flow cytometry samples and helping us with their analysis.



## **Table of Contents**

<b>Abstract</b> .....	<b>iii</b>
<b>Dedication</b> .....	<b>v</b>
<b>Acknowledgements</b> .....	<b>vi</b>
<b>Table of Contents</b> .....	<b>vii</b>
<b>List of Figures and Tables</b> .....	<b>ix</b>
<b>Figure Contributions</b> .....	<b>x</b>
<b>Abbreviations</b> .....	<b>xi</b>
<b>Chapter 1: Introduction</b> .....	<b>1</b>
The structure and function of the skin .....	1
UVR causes skin cancer.....	5
UV-induced DNA damage in the skin .....	6
DNA damage repair and the role of CDC25A on cell cycle regulation.....	8
Failure of DNA repair mechanisms leads to mutations .....	12
CDC25A is overexpressed in cancer .....	13
Significance.....	16
<b>Chapter 2: Materials and Methods</b> .....	<b>22</b>
Animals .....	17
Immunoblotting.....	18
Immunofluorescence, histochemistry, and morphometric analysis .....	19
Flow cytometric analysis .....	20
Southwestern assays.....	21

Statistical analyses .....	22
<b>Chapter 3: Results.....</b>	<b>24</b>
Development of skin targeted <i>Cdc25a</i> mutant mice .....	24
Elimination of DNA damage is accelerated in UV-exposed <i>Cdc25a</i> mutant skin .....	25
S-phase and G <sub>2</sub> /M cells are increased in UV-irradiated <i>Cdc25a</i> mutant skin.....	28
Apoptosis is increased in <i>Cdc25a</i> mutants following UV exposure.....	31
Ablation of <i>Cdc25a</i> alters the kinetics of epidermal hyperplasia following UV exposure .....	32
Deletion of <i>Cdc25a</i> does not alter the number of UV-induced tumors, but alters tumor growth .....	34
<b>Chapter 4: Discussion .....</b>	<b>39</b>
<b>References.....</b>	<b>45</b>

## List of Figures and Tables

<b>Chapter 1: Introduction .....</b>	<b>1</b>
<b>Figure 1. Anatomy of mouse skin.....</b>	<b>1</b>
<b>Figure 2. Common forms of DNA damage resulting from UV-irradiation in the skin.....</b>	<b>7</b>
<b>Figure 3. DNA damage response pathways involving CDC25A and p53 as signal transducers.....</b>	<b>11</b>
<b>Figure 4. Potential mechanism for CDC25A regulation of DNA damage repair, mutagenesis and proliferation following UV-induced DNA damage .....</b>	<b>16</b>
<b>Chapter 2: Materials and Methods .....</b>	<b>17</b>
<b>Table 1. Primer sequences used for genotyping.....</b>	<b>17</b>
<b>Chapter 3: Results.....</b>	<b>24</b>
<b>Figure 5. Generation of <i>Cdc25a</i> knockout mouse.....</b>	<b>24</b>
<b>Figure 6. Experimental model: timeline of UV-irradiation and euthanasia of mice.....</b>	<b>25</b>
<b>Figure 7. Removal of DNA adducts is accelerated in <i>Cdc25a</i> mutant compared to control skin.....</b>	<b>27</b>
<b>Figure 8. UV-induced proliferation is unchanged in <i>Cdc25a</i> mutant skin compared to control skin.....</b>	<b>29</b>
<b>Figure 9. Flow cytometry reveals subtle cell cycle differences in <i>Cdc25a</i> control and mutant skin following UV.....</b>	<b>30</b>
<b>Figure 10. Cell death is increased in <i>Cdc25a</i> mutant skin at 18 h following UV-irradiation ...</b>	<b>32</b>
<b>Figure 11. Hyperplasia is increased in <i>Cdc25a</i> mutant skin at 36 h post-UV.....</b>	<b>34</b>
<b>Figure 12. Experimental model for Tg.AC<sup>+</sup>/<i>Cdc25a</i> tumorigenesis experiment.....</b>	<b>35</b>

<b>Figure 13.</b> Tumor incidence and multiplicity are similar between Tg.AC <sup>+</sup> / <i>Cdc25a</i> mutant and control mice. ....	37
<b>Figure 14.</b> UV-induced tumor development is altered in Tg.AC <sup>+</sup> / <i>Cdc25a</i> mutant compared to control mice .....	38

## Figure Contributions

Jenan AlMatouq	Flow cytometry in paraffin-embedded tissue sections (Figure 9A, B, C and Figure 10C)
Michaela Behrens	Cyclopyrimidine dimer immunofluorescence (Figure 7A) and TUNEL assay and quantification (Figure 10A,B)
Patrick Carroll	Tg.AC <sup>+</sup> /Cdc25a tumor volume measurements (Figure 14B, D)
Brianna Hammiller	BrdU immunofluorescence and quantification (Figure 8A,B)
Dr. Laura Hansen	Hyperplasia and epidermal thickness measurements (Figure 11B, C) and hematoxylin and eosin images (Figure 11A)
Dr. Susan Repertinger	Histopathological characterization of tumor samples (Figure 14C)

## **Abbreviations**

<b><u>Abbreviation</u></b>	<b><u>Description</u></b>
53BP1	p53 binding protein 1
6-4 PP	Pyrimidine (6-4) Pyrimidone Photoproducts
8-oxo-dG	8-oxo-deoxyguanosine
AALAC	American Association of Laboratory Animal Care
AK	Actinic Keratosis
ANOVA	Analysis of Variance
ASK-1	apoptosis signal regulating kinase 1
ATM	Ataxia Telangiectasia Mutated
ATRIP	ATR Interacting Protein
ATR	Ataxia Telangiectasia mutated and Rad3 related
BCC	Basal Cell Carcinoma
BER	base excision repair
BrdU	Bromodeoxyuridine
BSA	bovine serum albumin
C	cytosine
CDC25	Cell Division Cycle 25

CDK	Cyclin Dependent Kinase
CPD	Cyclobutane Pyrimidine Dimer
DAPI	4',6-diamidino-2-phenylindole
DNA	Deoxyribonucleic Acid
DSBs	double strand breaks
d.p.c	days post-coitum
E	embryonic
EGFR	Epidermal Growth Factor Receptor
h	hour
kJ	kilo joule
HCC	Hepatocellular Carcinoma
m	meter
M	Mitosis
MAPK	mitogen-activated protein kinase
mRNA	messenger ribonucleic acid
MDC1	mediator of DNA damage checkpoint 1
NER	nucleotide excision repair

NMSC	non-melanoma skin cancer
PBS	Phosphate Buffered Saline
PCNA	proliferating cell nuclear antigen
PCR	polymerase chain reaction
PI3K	phosphoinositide 3-kinase
PTP	protein tyrosine phosphatases
PUMA	p53 upregulated modulator of apoptosis
Rad17-RFC	Rad17-Replication Factor C
ROS	reactive oxygen species
RPA	Replication Protein A
S	Synthesis
SAPK	stress activated protein kinase
SK	solar keratosis
ssDNA	single-stranded DNA
T	thymine
TBS-T	Tris-Buffered Saline Tween-20
TopBP1	topoisomerase binding protein



Tg.AC	v-ras <sup>Ha</sup> transgenic mouse line
TUNEL	Terminal Deoxynucleotidyl Transferase dUTP Nick End Labeling
UV	Ultraviolet
UVA	Ultraviolet A
UVB	Ultraviolet B
UVC	Ultraviolet C
UVR	Ultraviolet Radiation

## Chapter 1: Introduction

### The structure and function of the skin

The skin and its derivatives comprise the integumentary or “covering” system of our bodies <sup>1</sup>. About 16% of our body weight is composed of the skin, which is the largest organ. The epidermis and dermis are the two primary components of the skin, with the hypodermis or superficial fascia being the region consisting of connective tissue and adipose tissue (Figure 1). Structures associated with the skin include sweat and sebaceous glands, hair, and nails. Moreover, skin cells contain pain receptors to alert the nervous system when possible damage has occurred. The epidermis of the skin is the component which defines its characteristic qualities.

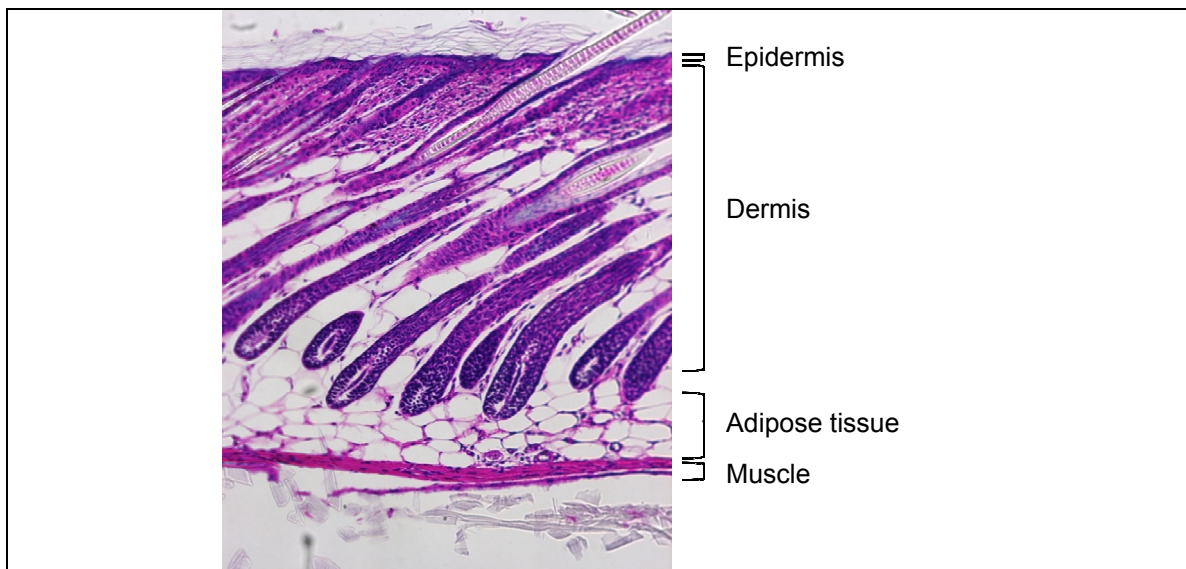


**Figure 1. Anatomy of mouse skin**

Mouse skin is composed of the keratinized stratified squamous epidermis and the underlying dermis, which consists mostly of dense irregular connective tissue and housing hair follicles. Adipose and connective tissue underlying the dermis compose the hypodermis.

The epidermis is a squamous epithelium derived from the ectoderm and is composed primarily of stratified layers of keratinocytes, which is unique in its ability to become keratinized and thus protected from the assaults of the environment<sup>2</sup>. The epidermis contains 18 types of keratin intermediate filaments<sup>3</sup>. Because the epidermis is a stratified epithelium, each stratum is characterized by the proteins they express as well as the shape of their cells. The strata of the epidermis are subdivided into 5 layers. From deepest to most superficial, they are: stratum basale (basal layer), stratum spinosum (spinous layer), stratum granulosum (granular layer), stratum lucidum, and stratum corneum (cornified layer). Mouse and human epidermis are avascular and have no blood supply of their own<sup>4</sup>. Nutrients are supplied to the epidermis by transfer from the dermis through the dermal papillae present at the junction between the dermis and the basal layer (stratum basale) of the epidermis. The dermal papillae increase the surface area between the upper dermis and epidermis, increasing transfer of oxygen, nutrients, and waste. Other cells present in the epidermis include Langerhans (antigen-presenting) cells, dendritic epidermal T-cells, Merkel (neuroendocrine) cells, and melanocytes in humans (pigment-forming)<sup>1,5</sup>. The epidermis is innervated by free nerve endings originating from the subepidermal nervous plexus<sup>6</sup>.

The basal layer of the epidermis, consisting of cuboidal or columnar cells, is the least differentiated and in mouse skin is normally the only mitotically active stratum. The cytoskeleton of basal cells is characteristically comprised of intermediate filaments Keratin 14 and Keratin 5<sup>3</sup>. Keratin 14 and Keratin 5 are associated with maintenance of a high proliferative capacity<sup>3</sup>. Basal keratinocytes are polar with hemidesmosomes found at the basement membrane of basal keratinocytes<sup>7</sup>. Integrins of the hemidesmosomes bind

components of the extracellular matrix such as laminin, collagen, and fibronectin to the basal cells<sup>8</sup>. Desmosomes are localized within the apical region or apical membrane of basal keratinocytes, and are also found in all nucleated layers of the epidermis<sup>9-11</sup>. Desmosomes are comprised of two mirror-image plaques that link to the intermediate filaments beneath the plasma membrane<sup>12,13</sup>. Adherens junctions are also found in all the nucleated cells of the epidermis<sup>14</sup>, composed of cadherin and other associated proteins. Basal keratinocytes are able to divide both symmetrically and asymmetrically<sup>15</sup>. When basal cells divide asymmetrically, which occurs during epidermal differentiation in mature skin, one daughter cell has the ability to stay attached to the basement membrane while the other loses contact and migrates up into the suprabasal spinous layer<sup>15,16</sup>. In order to achieve this stratification, the plane of the mitotic spindle is oriented perpendicular to the basement membrane<sup>11</sup> such that one daughter cell will be oriented suprabasally. In this transition into the suprabasal layers, the cells begin to express Keratin 1 and Keratin 10 filament bundles, which have been associated with epithelial stratification<sup>3</sup>.

As the cells of the spinous layer move towards the surface of the skin to form the granular layer, they begin to produce keratohyalin granules that contain the protein profilaggrin. When profilaggrin is processed into filaggrin, it creates bundles of keratin filaments producing macrofibrillar cables. Cornified envelope proteins also aid in adding strength to the granular layer as they activate the enzyme transglutaminase, which crosslinks glutamine and lysine. These crosslinks stabilize and hold together the keratin microfibrils<sup>14</sup>. Cells of the granular layer contain lipid-filled lamellar bodies, which release their contents into the extracellular space. This release of lipid into the

extracellular space contributes to the formation of a permeability barrier<sup>17</sup>. Tight junctions are found in the spinous and granular layers of the epidermis<sup>11</sup>. Like adherens junctions, tight junctions form a continuous belt of adhesion between cells of the epidermis, but they seal the membranes of adjacent cells together and prevent liquid from passing through to the lower layers of the skin and inside the body<sup>12,18</sup>.

As the cells in the granular layer continue to differentiate, the nucleus and other organelles are destroyed. These cells become anucleate as they form the cornified layer. The stratum corneum forms a waterproof seal as the keratin filaments are crosslinked by disulfide bonds and membrane lipids from the granular layer are exocytosed, creating a layer with high lipid content on the surface of the skin.

In contrast to the highly keratinized epidermis, the dermis (Figure 1) consists primarily of dense irregular connective tissue, which is composed of collagen, elastin, and glycosaminoglycans. The dermis provides structural support to the skin, creates elasticity and plasticity of the skin, and aides in the immunological support of the epidermis. Hair follicles and associated sebaceous glands are found in the dermis, as well as sweat ducts and nerve processes<sup>19,20</sup>. Also within the dermis are blood vessels, which provide vascular supply for sweat glands, hair follicles, and all other cells<sup>21,22</sup>. Blood vessels of the dermis are composed primarily of endothelial cells, which are important for immune response, skin homeostasis, temperature regulation, and wound healing. The dermis also contains macrophages, monocytes, and fibroblasts. In mice, the dermis and subcutaneous tissue are separated by a layer of striated skeletal muscle<sup>22</sup>, which is absent in human skin except on the back of the neck<sup>19</sup>. The presence of melanocyte-generated melanin and pigmented hair in human and mouse skin, respectively, aids in protection

from sun exposure. The keratinized epidermis and collagenous dermis together serve as a barrier from the elements by both repelling penetration of noxious substances from outside the organism and by preventing water and heat loss.

### **UVR causes skin cancer**

One of the most serious assaults on the skin is from overexposure to UVR in the form of sunlight. UVR exposure causes most non-melanoma skin cancer (NMSC), which is the most common type of cancer in the United States and in fair-skinned populations<sup>23,24</sup>. Repeated exposure to UV-irradiation is dangerous because it causes DNA damage in the cells of the epidermis, resulting in mutations and genomic instability. From 1992 to 2006, the number of skin cancer procedures increased by 76.9% (about a 4.2% increase each year)<sup>24</sup>. However, the increase in NMSC cases is most likely due partially to the increasing age of the population as well as increasing exposure to the sun<sup>25</sup>. Although individual cases are not as expensive to treat when compared to the treatment of other cancer types<sup>24</sup>, NMSC was the fifth most expensive cancer overall within Medicare recipients. From 1992 to 2006, the total number of NMSC treatment procedures increased by 77% from 1,158,298 to 2,048,517 in 2006<sup>24</sup>. Moreover, it consumes 4.5% of all Medicare cancer expenses combined<sup>24</sup>.

NMSC includes both basal and squamous cell carcinomas, which together account for 95% of NMSCs<sup>23</sup>. It is estimated that about 2,000 people die each year in the United States of NMSC<sup>26</sup>. Most of the deaths are due to metastasis of squamous cell carcinoma. Some rare deaths are due to basal cell carcinomas that invade vital organs. Risk for acquiring NMSC is inversely proportional to skin pigmentation and thus fair-

skinned individuals are at higher risk. The higher risk for fair-skinned individuals is due to their decreased protection by melanin production in the basal layer of the epidermis.

Squamous cell carcinoma (SCC) is the second most common malignancy after basal cell carcinoma (BCC) in humans. Increased exposure to UV correlates directly with increased risk of developing SCC and BCC. Actinic keratosis (AK) is the progenitor to many SCCs and is also more common in individuals who have had high cumulative exposure to UVR. SCC develops most commonly in areas regularly exposed to the sun, such as the head, face, and back of the hands.

### **UV-induced DNA damage in the skin**

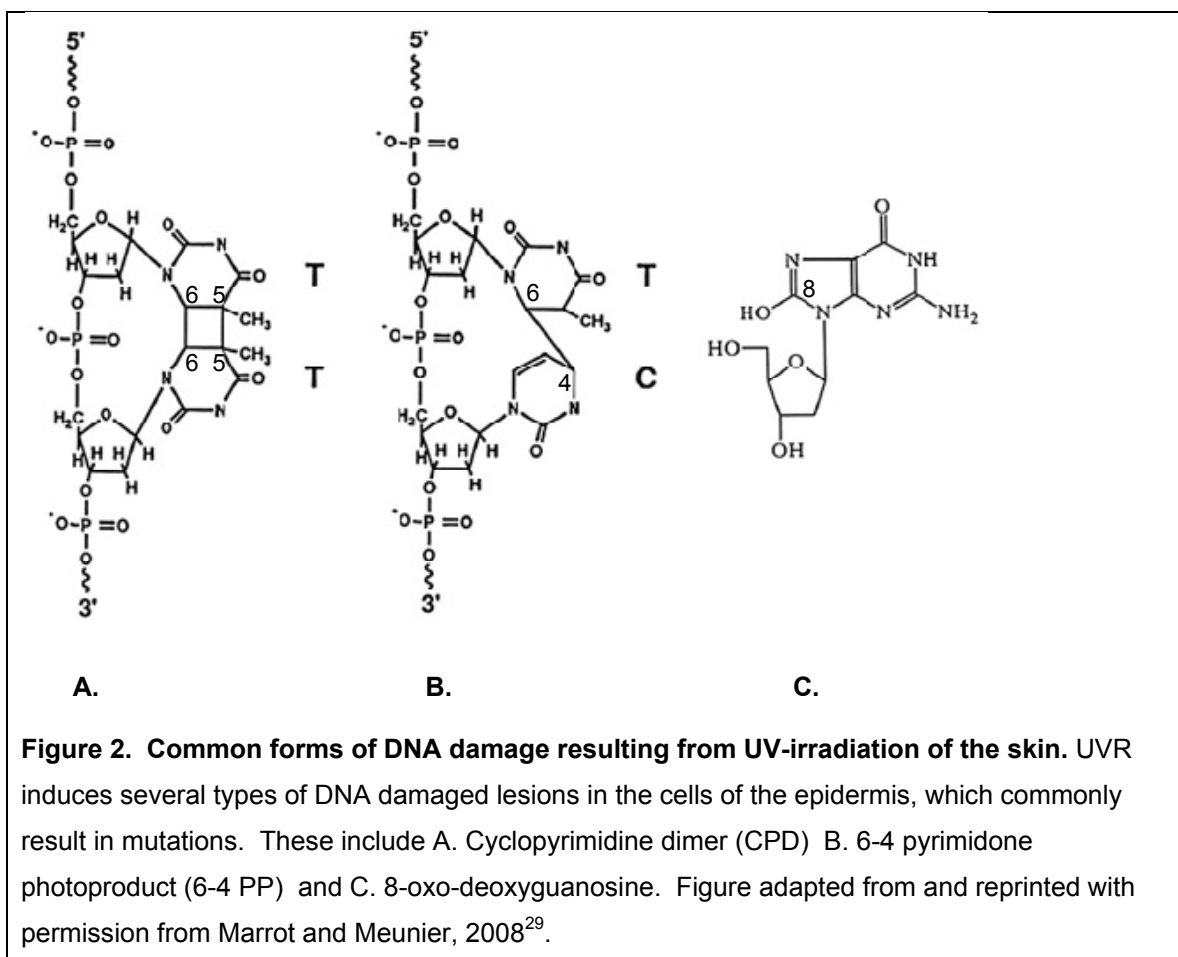
Chronic exposure to UVR, primarily UVB and to a lesser extent UVA, is the major cause of melanoma and non-melanoma skin cancer because of its DNA damaging capabilities. Ultraviolet radiation (UVR) consists of 3 wavelengths, ultraviolet A (UVA) (320-400 nm), ultraviolet B (UVB ) (280-320 nm) and ultraviolet C (UVC) (below 280 nm). UVA makes up 6.3% of the sun's emission. Only 1.3% is composed of UVB, although it is the highest energy radiation to reach the surface of the earth. The ozone layer absorbs most, if not all, UVC rays, protecting life at the surface of the earth from this harmful radiation. UVB and to a lesser extent, UVA cause most of the DNA damage. Interestingly, the skin contains several chromophores, including DNA (nucleic acids), proteins (aromatic amino acids), melanin, and urocanic acid<sup>1</sup>. The nucleic acids in DNA contain many conjugated ring structures<sup>27</sup>. Thus, DNA in skin cells readily absorbs UVR and is highly susceptible to forming photoproducts. The epidermis of the skin absorbs UVB irradiation and only 10-20% is able to reach the basal layer of human skin after being absorbed into the suprabasal cells<sup>28</sup>. The longer wavelength and thus lower

energy of UVA penetrates more deeply into the dermis of the skin<sup>29</sup> and has been found to contribute to DNA damage but also contributes to aging and reactive oxygen species production.

Exposure to UVB causes damage to DNA in the skin in the form of cyclobutane pyrimidine dimers (CPDs) (Figure 2A), pyrimidine 6-4 pyrimidone photoproducts (6-4PPs) (Figure 2B), Dewar isomers, and thymine glycols<sup>30</sup>. CPDs are formed when C5 and C6 carbons on adjacent pyrimidines form covalent bonds. Alternatively, 6-4 PPs are formed by bond formation between C4 and C6 carbons on adjacent pyrimidines. CPDs have been found to be the cause of most UV-induced mutations<sup>31</sup>. Because CPDs create bulky lesions in the structure of DNA, they can hinder DNA replication, transcription, and even cell division<sup>29</sup>.

Another type of UV-induced DNA damage occurs through the production of reactive oxygen species (ROS) following UVA and, to a lesser extent, UVB irradiation. The damage resulting from UVA exposure includes DNA single strand breaks, DNA to protein crosslinks, and a small number of directly produced CPDs<sup>32</sup>. UVA is absorbed mostly by chromophores other than DNA in the skin, such as porphyrins and quinones<sup>29</sup>. These chromophores produce ROS that can interact with DNA, leading to damage and mutagenesis. Increasing evidence suggests that the immunosuppressive effects of ROS cause conversion of solar keratoses (SKs) to squamous cell carcinoma<sup>33</sup>. A well-known biomarker of oxidative stress is the 8-oxo-deoxyguanosine (8-oxo-dG) adduct (Figure 2C) which was first isolated from the urine of human and mouse in 1989<sup>34,35</sup>. The 8-oxo-dG adduct results from oxidation of guanosine.





### DNA damage repair and the role of CDC25A in cell cycle regulation

As described earlier, UV-induced DNA damage in the skin is the primary cause of mutations leading to tumorigenesis. Damaged DNA in the form of CPDs and 8-oxo-dG adducts in mammalian skin cells is repaired by nucleotide excision and base excision repair, respectively. The first step in the DNA damage response is damage recognition or sensing. The 9-1-1 complex, comprised of Rad9, Rad1, and Hus1 proteins, has a PCNA-like structure and is immediately recruited to the site of damage by the Rad17-Replication Factor C (Rad17-RFC) complex<sup>36</sup>.

Previously, it was thought that Ataxia telangiectesia mutated (ATM) and ATM and Rad3 Related (ATR) proteins were only mediators activated by Rad sensor proteins.

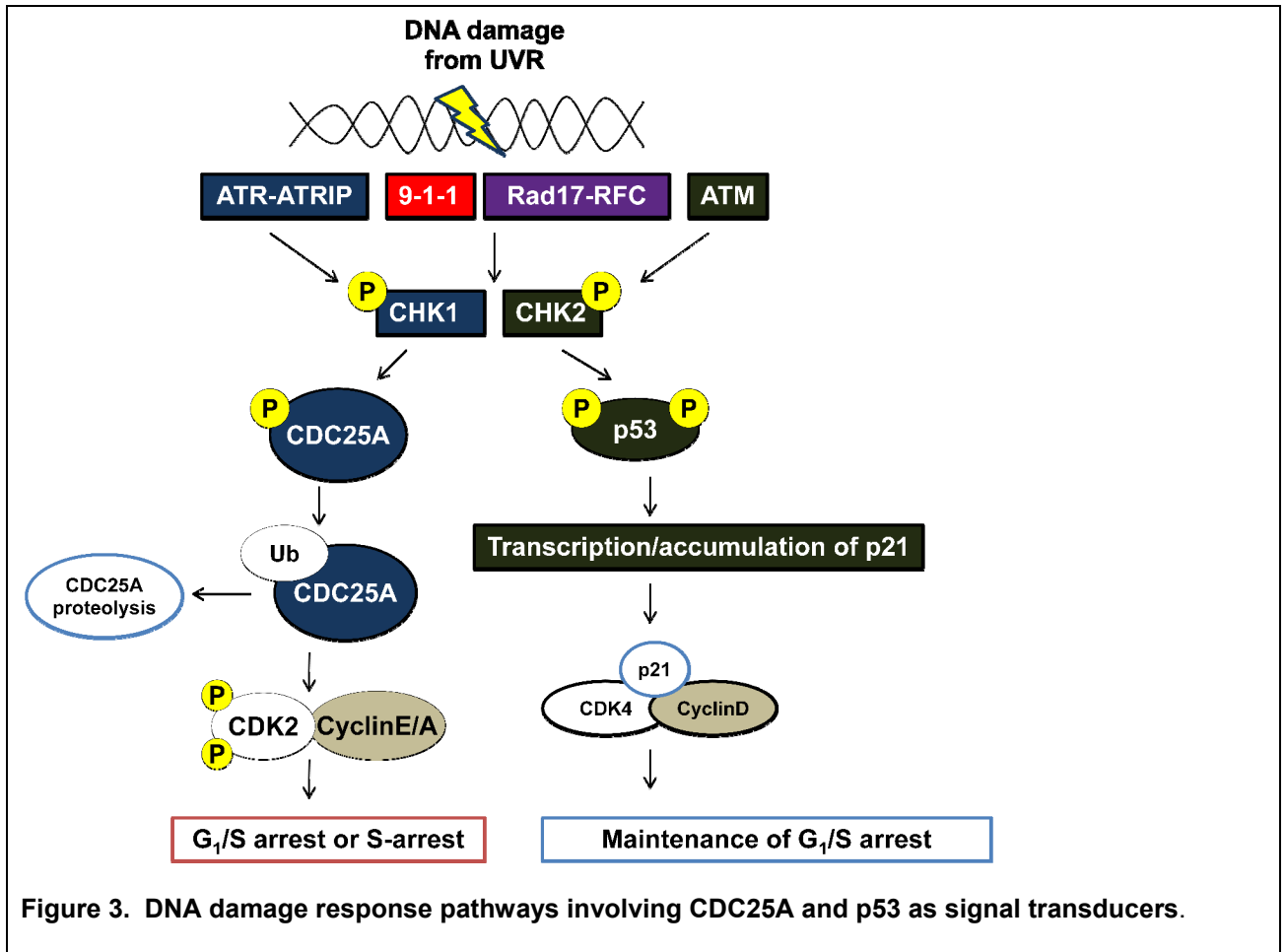
However, more recent evidence suggests that ATM and ATR might have the ability to bind the DNA preferentially in response to damaging agents, such as ionizing radiation and UVR<sup>37</sup> (Figure 3). Nevertheless, there is mixed evidence supporting this theory. ATM is recruited primarily in response to ionizing radiation which causes double strand breaks (DSBs). ATR is activated by UV irradiation and is recruited to DSBs, stalled replication forks and sites of damaged bases<sup>38</sup>, which all produce single-stranded DNA coated with Replication protein A (RPA-coated ssDNA)<sup>39</sup>. Evidence suggests that ATR binds preferentially to regions containing UV-induced damage, such as 6-4 PPs<sup>40</sup>. ATR interacts with the ATR Interacting Protein (ATRIP)<sup>36</sup>, which associates with ssDNA.

The mediator molecules activated by ATM or ATR in humans are similar in that they all have conserved BRCT domains (the carboxyl terminal domain on Breast Cancer Gene 1), which are found in many proteins involved in the DNA damage response and play a role in mediating protein-protein interactions<sup>37</sup>. In humans, mediator molecules include p53 binding protein (53BP1), topoisomerase binding protein (TopBP1) and mediator of DNA damage checkpoint 1 (MDC1). These mediators phosphorylate and thus activate the transducers, Chk1 and Chk2<sup>36</sup>.

Chk1 and Chk2 are serine/threonine kinases that transduce the DNA damage signal by phosphorylation of effector molecules Cell Division Cycle 25 (CDC25) and p53<sup>36</sup>. Chk2 is phosphorylated primarily by ATM, while Chk1 is phosphorylated primarily by ATR<sup>36</sup>. Cell cycle checkpoints activated by signaling pathways downstream from these effectors can halt the cell cycle at any of the G<sub>1</sub>/S, intra-S, and G<sub>2</sub>/M transitions to allow time for DNA repair before resumption of cell division. In response to damage caused by UV-irradiation, keratinocytes undergo p53-dependent arrest in G<sub>1</sub>,

S, or G<sub>2</sub><sup>41,42</sup>, allowing for adequate time for DNA damage repair mechanisms to take place.

In response to UV, ATR is activated and phosphorylates Chk1, activating it and leading to the phosphorylation of CDC25A, which is then targeted for ubiquitin-mediated degradation by the proteasome (Figure 3). CDC25A is a dual specificity phosphatase<sup>43</sup> that removes inhibitory phosphate groups from Cyclin Dependent Kinase 2 (CDK2). CDK2 forms a complex with cyclin E to move the cell through the G<sub>1</sub>/S checkpoint into S-phase. CDK2 also forms a complex with cyclin A, allowing progression through the S-phase, or intra-S checkpoint of the cell cycle. Thus, removal of the inhibitory phosphates on CDK2 by CDC25A allows for activation of the CDK2-Cyclin E complex and the CDK2-Cyclin A complex, enabling advancement into and progression through S-phase. Degradation of CDC25A stalls the cell in G<sub>1</sub>/S and/or S-phase and DNA replication initiation is halted. This provides time necessary for mechanisms such as nucleotide excision repair and base excision repair to repair the DNA prior to fixation of DNA damage upon DNA replication.



UV-irradiation can also suppress DNA damage response checkpoints through activation of receptor tyrosine kinase signaling. For example, UV-irradiation activates the epidermal growth factor receptor family of tyrosine kinase receptors through reactive oxygen species inactivation of protein tyrosine phosphatases<sup>44</sup>. Three of four EGFR family members are expressed in the skin, including EGFR (ErbB1), ErbB2, and ErbB3. Studies in our laboratory suggest that activation of ErbB2 by UV irradiation leads to increased activation of the phosphoinositide 3-kinase (PI3K)/Akt signaling pathway, which suppressed activation of Chk1<sup>45</sup>. Specifically, PI3K has been shown to inhibit Chk1 activation, which in turn prevents the ubiquitin-mediated degradation of CDC25A,

preventing arrest of the cell cycle<sup>46</sup>. Without cell cycle arrest, DNA damage is unrepaired, leading to mutations in DNA and tumorigenesis increases.

### **Failure of DNA repair mechanisms leads to mutations**

If UV-induced DNA damage is not repaired, mutations can result. The majority of mutations are C → T transitions and CC→TT transitions, known to be signatures of UV-irradiation resulting from CPDs<sup>47</sup>. This occurs only when cytosine is adjacent to either another pyrimidine (thymine or cytosine)<sup>47,48</sup> and can produce a CC→TT mutation. By far the most common mutations in skin tumors are in the *Trp53* tumor suppressor gene. At least 50% of invasive squamous cell carcinomas have p53 mutations<sup>47</sup>. Most of these mutations occur at the sites where the UV-signature CPDs are formed<sup>49,50</sup>.

The presence of 8-oxo-dG adducts resulting from ROS results in a 2% mutation rate in human cells transfected with plasmids containing a single 8-oxo-dG adduct<sup>51</sup>. Point mutations at both the oxidized guanine itself and at the base adjacent to the 8-oxo-dG have been found on codon 12 of the *c-ras<sup>Ha</sup>* protooncogene in mammalian cells<sup>52</sup>. When ROS-induced mutations occur on protooncogenes, such as *c-ras<sup>Ha</sup>*, oncogene activation can occur. DNA repair mechanisms are crucial in preventing DNA damage from leading to cancer development. Studies have shown that up to forty-six percent of squamous cell carcinomas have mutations in the *ras* gene<sup>53-56</sup>. The *ras* proto-oncogene family consists of Harvey *ras* (*ras<sup>Ha</sup>*), Kirsten *ras* (*ras<sup>Ki</sup>*) and neuroblastoma *ras* (*ras<sup>N</sup>*)<sup>57</sup>. Mutations in all 3 *ras* family members have been found in SCC, however, mutations in *ras<sup>Ha</sup>* are the most common<sup>56</sup>. Activation of *ras* triggers the initiation of the Raf/Mek/Mitogen activated protein kinase (MAPK) signal transduction pathway, which induces transcription of genes through activator protein 1 (AP-1) and other transcription

factors. Mutation and thus activation of the *ras* protooncogene can lead to overproduction of the proteins involved in cell growth and proliferation thus contributing to tumor initiation<sup>58,59</sup>.

Researchers have taken advantage of the fact that activation of the c-*Ras*<sup>Ha</sup> protooncogene correlates with tumor initiation by creating a mouse in which the activation of *Ras*<sup>Ha</sup> has already been accomplished. The transgenic Tg.AC mouse, which contains multiple copies of the *v-Ras*<sup>Ha</sup> oncogene, is genetically initiated to develop skin tumors in response to tumor promoters such as UV-irradiation or chemical promoters such as 12-O-tetradecanoylphorbol 13-acetate (TPA). The Tg.AC mouse was utilized in this thesis as a model for better understanding the role of CDC25A in UV-induced tumor development.

### **CDC25A is overexpressed in cancer**

NMSC develops as a result of both mutations in key regulatory genes as well as overexpression of genes involved in cell cycle regulation and cell proliferation. Overexpression of the protein phosphatase CDC25A, described earlier, is often found in combination with inactivation of the p27<sup>KIP1</sup> inhibitor of CDK-Cyclin complexes<sup>60</sup>. p27 specifically binds and targets the CDK2/Cyclin E complex for proteasomal degradation<sup>61</sup>. Because p27 controls progression through the cell cycle, it plays an important role in prevention of cancer and unregulated proliferation. Moreover, overexpression of CDC25A often correlates with increased malignancy and poor prognosis. The impact of CDC25A overexpression in particular is seen in hepatocellular carcinoma (HCC) where the protein is overexpressed in 78% of HCC as compared to only 20% overexpression of CDC25B<sup>62</sup>. In this model CDC25A increase was associated with disease relapse.

CDC25 protein tyrosine phosphatases are found in all eukaryotic organisms except plants and are conserved regulators of the cell cycle. Protein tyrosine phosphatases (PTPs) all contain a unique CX<sub>5</sub>R catalytic motif. The cysteine residue of this signature PTP signature motif acts as a nucleophile, attacking phosphate groups on CDKs and forming a phosphorylcysteine intermediate<sup>63</sup>. Thus, CDC25s are responsible for removing inhibitory phosphates placed on positions 14 and 15 of CDKs by Wee and Myt kinases<sup>64</sup>. Moreover, the CDC25s are considered “dual-specificity” phosphatases because they are able to remove phosphate groups from both serine/threonine kinases and tyrosine kinases<sup>65</sup>. Activation of CDK/cyclin complexes leads to cell cycle progression through each of the checkpoints. These checkpoints include G<sub>1</sub>/S, Intra S, G<sub>2</sub>/M, and the spindle assembly checkpoint<sup>66</sup>.

There are 3 known CDC25 homologs in mammals that include CDC25A, CDC25B, and CDC25C. As described earlier, one of the substrates of CDC25A is CDK2, which complexes with Cyclin E and Cyclin A to move the cell through the G<sub>1</sub>/S checkpoint and through the S-phase, respectively. *Cdc25a*-null mice are embryonic lethal during days E5 through E7<sup>67</sup>. *Cdc25b*- and *Cdc25c*-null mice are viable, suggesting that *Cdc25a* alone is required for embryogenesis and has the ability to compensate for *Cdc25b* and *Cdc25c*<sup>67</sup>.

Much work has been done to investigate the role of CDC25A in cancer<sup>68</sup>. In mammary epithelial cells transfected with CDC25A to induce constitutive overexpression, the DNA damage response is perturbed due to uncontrolled DNA replication. CDC25A overexpressing cells are able to bypass the cell cycle arrest required for adequate DNA damage repair, resulting in genomic instability as seen

through an increase in chromosomal breaks<sup>61</sup>. It is no surprise then, that CDC25A is overexpressed in multiple cancer types including breast, prostate, ovarian, thyroid and colorectal<sup>64</sup>.

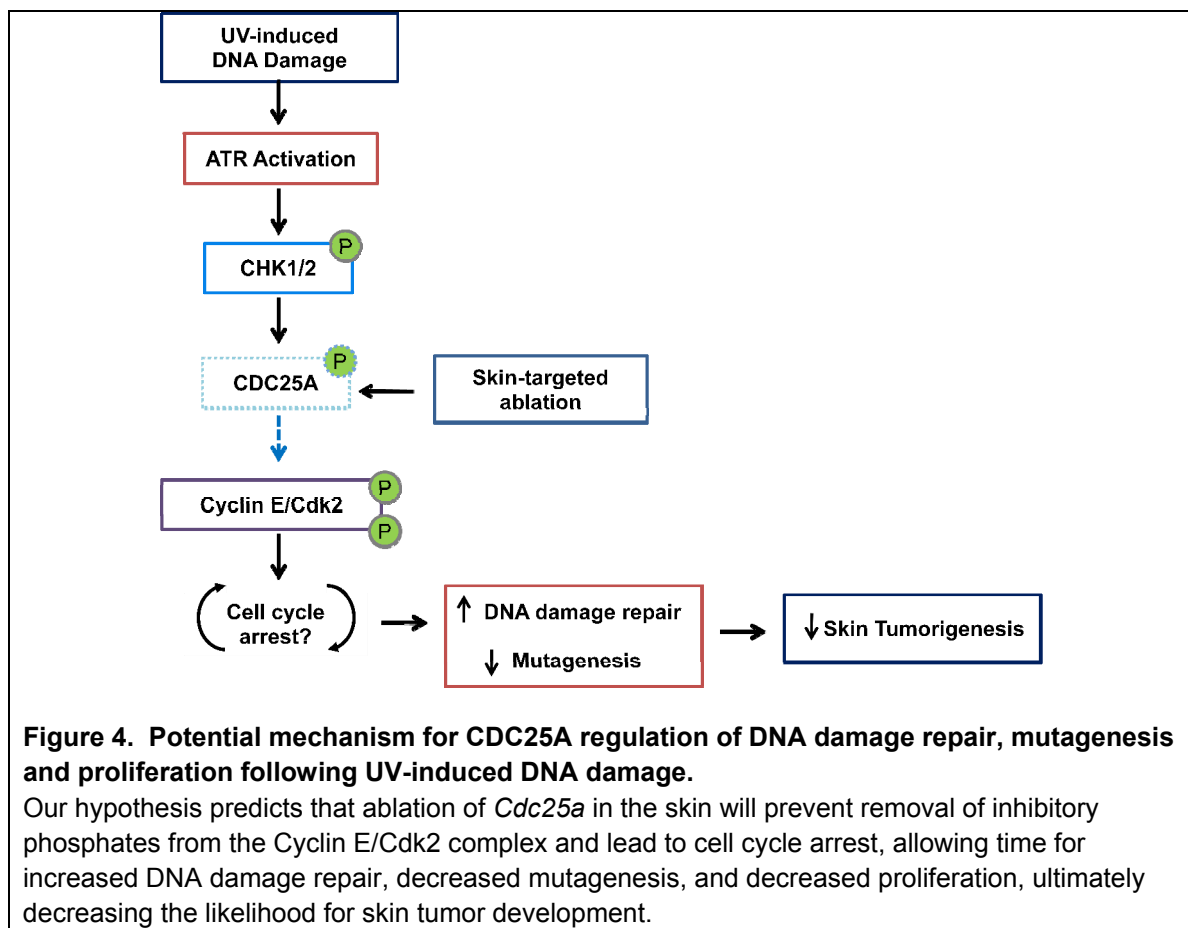
Aside from bypassing cell cycle arrest leading to genomic instability, CDC25A might have the ability to inhibit apoptosis, as it reduces the cell's response to oxidative DNA damage and stress, which is well-known to increase cancer risk<sup>69</sup>. For example, cells with induced expression of *Cdc25a* had decreased oxidative stress-induced apoptotic response<sup>69</sup>. CDC25A was also shown to directly inhibit activation of apoptosis signal regulating kinase 1 (ASK1), a protein responsible for the cell's response to reactive oxygen species, that causes cell death<sup>70</sup>.

Since CDC25A has been implicated both in inhibition of apoptosis and genomic instability, CDC25A is an attractive target for cancer therapy. Inhibitors for CDC25A have been synthesized based on the structure of Vitamin K. Vitamin K analogs inhibit protein tyrosine phosphatases (PTPs) by alkylation of the active site cysteine involved in their catalysis<sup>71</sup>. The compound with the greatest PTP inhibition thus far is Cpd 5. It was shown that Cpd 5 induces the phosphorylation and thus activation of ERK1/2, which correlates with inhibition of cell growth<sup>72</sup>. Experiments using Cpd 5 on rat hepatocellular carcinoma cells and MCF-7 breast cancer cells resulted in growth inhibition in vitro<sup>73,74</sup>. Using a transplantable hepatoma model in which injection of JM-1 cells causes tumor growth either subcutaneously or in the liver, animals treated with Cpd 5 had significant inhibition of tumor growth.



## Significance

CDC25A plays a major role in regulation of the cell cycle, DNA damage response and apoptosis. The role of CDC25A in non-melanoma skin cancer is currently unknown, yet appears to be a promising target for skin cancer therapy. Because of its role in the cell cycle, we hypothesized that ablation of CDC25A in the skin would increase cell cycle arrest following UV irradiation, allowing for improved repair of DNA damage and decreased skin tumorigenesis (Figure 4).



## Chapter 2: Materials and Methods

### *Animals*

*Cdc25a*<sup>fl/fl</sup> mice with *loxP* sites inserted flanking exons 1-3 of the *Cdc25a* gene were developed as described in Lee, et al.<sup>75</sup>. *Cdc25a*<sup>fl/fl</sup> mice were crossed with *Krt14* promoter-driven transgenic mice on an FVB/N background (The Jackson Laboratory, Bar Harbor, ME) and progeny backcrossed to generate skin-targeted *Cdc25a* knockouts (*Cdc25a*<sup>fl/fl</sup> *Cre*<sup>+</sup>) and their littermate controls (*Cdc25a*<sup>fl/fl</sup> *Cre*<sup>-</sup>). *v-ras*<sup>Ha</sup> transgenic Tg.AC mice on an FVB/N background were crossed with the *Cdc25a* mutants to produce Tg.AC<sup>+</sup> *Cdc25a* mutants (*Cdc25a*<sup>fl/fl</sup>/*Cre*<sup>+</sup>/Tg.AC<sup>+</sup>) and controls (*Cdc25a*<sup>fl/fl</sup>/*Cre*<sup>-</sup>/Tg.AC<sup>+</sup>). Genotyping was performed by PCR using the primers listed in Table 1.

**Table 1. Primer sequences used for genotyping.**

Two sets of primers were used for the *Krt14-Cre* PCR. One set (blue) was used to produce a positive-control band to ensure that the reaction was successful when the *Krt14-Cre*<sup>+</sup> band was absent. (F, forward sequence; R, reverse sequence)

Gene	Orientation	Primer Sequence
<i>Cdc25a</i>	F	5'-CAG AGC CTG AAG TCC TGT GAA GG-3'
	R	5'-CTG CCT AGT GTA GTT CCT ACA GCG-3'
<i>Krt14-Cre</i>	F	5'-ACC AGC CAG CTA TCA ACT CG-3'
	R	5'-TTA CAT TGG TCC AGC CAC C-3'
	F	5'-CTA GGC CAC AGA ATT GAA AGA TCT-3'
	R	5'-GTA GGT GGA AAT TCT AGC ATC ATC C-3'
<i>Tg.AC</i>	F	5'-ATT CTG AAG GAA AGT CC-3'
	R	5'-TGG ACA AAC TAC CTA CAG-3'

Animals were housed in the Creighton University Animal Facility, fed *ad libitum* with Purina lab chow and kept on a 12 hour light-dark cycle. All animal procedures were performed in accordance with American Association of Laboratory Animal Care

(AALAC) guidelines and approved by Creighton University Institutional Animal Care and Use Committee. Age matched *Cdc25a* mutant and control Tg.AC<sup>+</sup> mice were sham- or UV-irradiated once a week over a period of four weeks for a cumulative exposure of 4.3 kJ/m<sup>2</sup>. UV irradiation was generated using Ultraviolet B TL 40W/12 RS Bulbs (The Richmond Light Company, Richmond, VA) covered with Kodacel triacetate film to block UVC. The mice were exposed to approximately 30% UVA and 70% UVB, measured using Oriel Goldilux radiometric photodetector probes (Newport Corporation, Irvine, CA). Hair on the dorsal skin of the mice was clipped the day before UV-irradiation using a Wahl Animal clipper (Wahl Clipper Corporation, Sterling, IL) and close shaved with a Braun Series 3 shaver (Proctor and Gamble, Cincinnati, OH) just before exposure. Mice were placed under the lamps and exposed to between 0.5-1.3 kJ/m<sup>2</sup> UV each week. UV-induced dorsal skin edema was measured using a pocket thickness gauge with a fixed tension (Mitutoyo America Co., Aurora, IL). UV-exposed mice were euthanized 2, 12, 18, 36, or 72 hours following the final UV exposure or allowed to develop skin tumors and samples collected. Tumor samples were obtained at euthanasia when mice became moribund. Mice were injected with bromodeoxyuridine (BrdU, approximately 0.075 mg per gram body weight, Sigma-Aldrich, St.Louis, MO) one hour before euthanasia.

### ***Immunoblotting***

Epidermis was separated from the skin using the heat shock method<sup>76</sup> by briefly immersing the skin in a 58°C water bath and scraping off the epidermis. Protein was extracted from skin or epidermis by homogenizing in lysis buffer containing 10 mM Tris (pH 7.4), 150 mM sodium chloride (NaCl), 10% glycerol, 1% Triton X-100, 1 mM

EDTA, 1X Complete Protease Inhibitor Cocktail (Roche, Germany), 1 mM sodium orthovanadate ( $\text{Na}_3\text{VO}_4$ ), 1.5  $\mu\text{M}$  EGTA, and 10  $\mu\text{M}$  sodium fluoride ( $\text{NaF}$ ) using a motorized tissue homogenizer (Tissue Master 125, Omni International LLC, Bedford NH). Protein was quantified using the Coomassie Brilliant Blue G-250 protein assay (Bio-Rad, Hercules, CA) and equal amounts loaded onto 10% Tris-HCl polyacrylamide gels (Bio-Rad, Hercules, CA). Immunoblotting was performed using standard techniques with antibodies recognizing CDC25A (1:200 Santa Cruz, Santa Cruz, CA) or actin (Sigma-Aldrich, St.Louis, MO) in 3% bovine serum albumin (BSA) in phosphate buffered saline (PBS). Horseradish peroxidase-conjugated secondary antibodies (Cell Signaling, Beverly, MA), chemiluminescent reagents (Pierce, Rockford, IL), and autoradiography were used to visualize results. Ponceau S staining (Sigma-Aldrich, St.Louis, MO) and actin immunoblotting were used to confirm the evenness of loading and transfer. Densitometry was performed using 1DScan software (Scanalytics, Fairfax, VA).

#### ***Immunofluorescence, histochemistry and morphometric analysis***

Paraffin-embedded skin sections fixed in 10% neutral buffered formalin or 70% ethanol were deparaffinized with either xylene (Pharmco, Brookfield, CT) or Protocol Safe Clear (Fisher Scientific, Pittsburgh, PA) and rehydrated in a graded series of ethanol. Ethanol-fixed tissue sections were incubated in 2N hydrochloric acid and concentrated trypsin (one tablet per mL, Sigma-Aldrich, St.Louis, MO) before blocking in 10% normal goat serum (Vector Labs, Burlingame, CA) and incubating with antibodies recognizing BrdU (1:3, Becton Dickinson, Franklin Lakes, NJ) or CPD (1:1000, Kamiya Biomedical, Seattle, WA). The next day sections were washed in PBS and incubated in biotinylated

F(Ab)<sub>2</sub> fragment goat anti-mouse secondary (Jackson ImmunoResearch, West Grove, PA), followed by Texas Red Streptavidin (Vector Laboratories, Burlingame, CA) and 4',6-diamidino-2-phenylindole (DAPI) in mounting media consisting of 50% glycerol in PBS with 1.5 µg/mL DAPI (Molecular Probes, Invitrogen, Carlsbad, CA). Terminal transferase dUTP nick-end labeling (TUNEL) assay (Promega, Madison, WI) was performed following the manufacturer's protocol with formalin-fixed tissue. Controls for the immunofluorescence and TUNEL assays included incubating without the enzyme for the TUNEL assay and without the primary antibody for immunofluorescence assays. Photomicroscopy was performed using a Nikon microscope, a cooled camera and MagnaFire software (Olympus, Melville, NY) for image capture. Hematoxylin and eosin staining was performed using standard techniques. BrdU- and TUNEL-positive cells were quantified by counting all positively stained cells and the DAPI-positive basal cells in each section using a 20x objective. BrdU- and TUNEL-positive labeling indexes were calculated as the percentage of BrdU- or TUNEL-positive basal cells. Epidermal hyperplasia was measured by counting the number of nucleated epidermal cell layers and measuring the epidermal thickness in hematoxylin and eosin stained sections. Epidermal thickness was measured as the distance from the bottom of the basal layer to the top of the granular layer using digitally captured images. For each of these parameters, ten fields from each skin section were measured in randomly selected areas. For all morphometric analyses, the investigator was blinded as to the identity of the samples.

### ***Flow cytometric analysis***

Cell cycle analysis was performed by flow cytometry using *in vivo* skin samples. Two to four 50 µm sections were cut from formalin-fixed paraffin embedded blocks. The

sections were dewaxed with xylene and rehydrated with decreasing concentrations of ethanol (100%, 90%, 70%, 50%, and distilled water). Cells were then digested in 0.05% pepsin (Sigma) in PBS with pH 1.5 and incubated with Vindelov's Solution<sup>77</sup>. Flow cytometric analysis was performed in the Creighton Flow Cytometry Core Lab on the FACSCalibur flow cytometer (Becton Dickinson, Franklin Lakes, NJ) using the FL2 channel (585-42 bandpass filter). Single cells were identified by measuring area (FL2-A) and width (FL2-W) and data for at least 10,000 events for each sample were collected in list mode data files using Cell Quest Pro software (Becton Dickinson). A histogram for FL2-A intensity was plotted for single cells and cell cycle distributions were determined using CellQuest software (Becton Dickinson, Franklin Lakes, NJ).

### ***Southwestern assays***

CPDs and 8-oxo-dG adducts were detected by Southwestern assays. Dorsal epidermis was collected by liquid nitrogen scraping of flash frozen skin<sup>78</sup>. DNA was extracted from the epidermis by incubating in 1.5 mL of a tail solubilization buffer containing 200 µg per mL Proteinase K and 100 mM NaCl in 1x SET (10% SDS, 50 mM EDTA, 100 mM Tris (pH 8.0)) overnight at 37°C with shaking. The next day, 200 µL of a tail salt solution containing 4.21 M NaCl, 0.63 M KCl, and 10 mM Tris (pH 8.0) was added and DNA was precipitated using 2 volumes (3.4 mL) 100% ethanol overnight at 20°C. The next day, the pellet was washed with 1 mL of 80% ethanol and the DNA pellet collected by centrifugation. The pellet was resuspended in an elution buffer containing 0.4 mM NaOH and 0.1 mM EDTA. DNA was quantified using an ND-1000 spectrophotometer (NanoDrop, Wilmington, DE). DNA (0.25 µg) was heated to 95°C for 10 minutes and neutralized with an equal volume 2 M ammonium acetate before use. DNA (0.25 µg)

was blotted onto a nitrocellulose membrane and dried at 80°C for 1 hour to fix the DNA to the membrane. The baked membrane was rehydrated in Tris-Buffered Saline Tween-20 (TBS-T) (10 mL 10% Tween 20, 100mL 10x TBS and 890 mL deionized water) and blocked in 5% bovine serum albumin (BSA) in TBS-T for one hour before incubating in primary antibody (Anti-8-oxo-dG, 1:500, Japan Institute for Control on Aging, Shizuoka, Japan or Anti-Thymine Dimer, 1:500, Kamiya Biomedical Company, Seattle, WA) in 5% BSA/TBS-T overnight at 4°C. The next day, the membrane was washed in TBS-T before incubating in horse anti-mouse IgG horseradish peroxidase-linked secondary (1:10,000, Cell Signaling Technologies, Beverly, MA) in 5% BSA/TBS-T for 45 minutes at room temperature. The blot was washed 2 times in TBS-T and the signal was detected by incubation with 20x LumiGLO chemiluminescent Reagent and 20x Peroxide (1:1, Cell Signaling Technologies, Beverly, MA). The signal was detected using either a BioRad Chemidoc XRS+ (Bio Rad Life Science Research, Hercules, CA) or developed on Kodak BioMax Film (Carestream Health, Rochester, NY). Densitometry was performed using ImageLab software (Bio Rad Life Science Research, Rochester, NY).

### ***Statistical Analyses***

A Student's two-tailed *t*-test or two-way ANOVA were used to determine statistical significance.  $P \leq 0.05$  was considered to be significant.

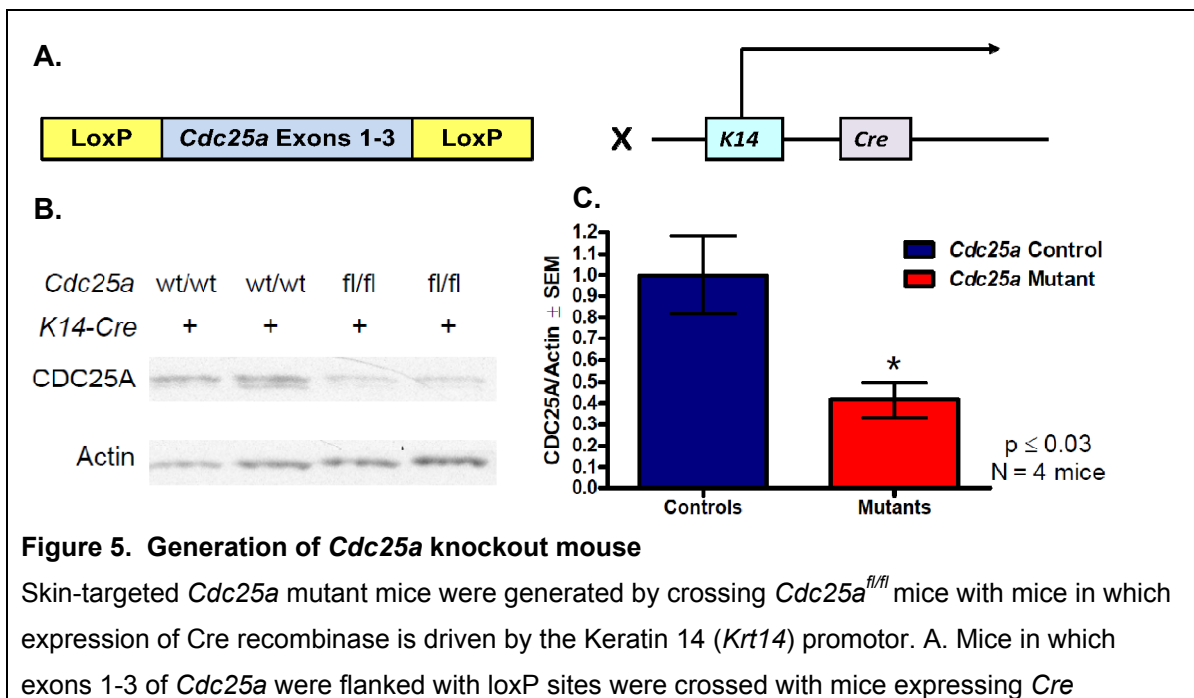




## Chapter 3: Results

### *Development of skin targeted Cdc25a mutant mice*

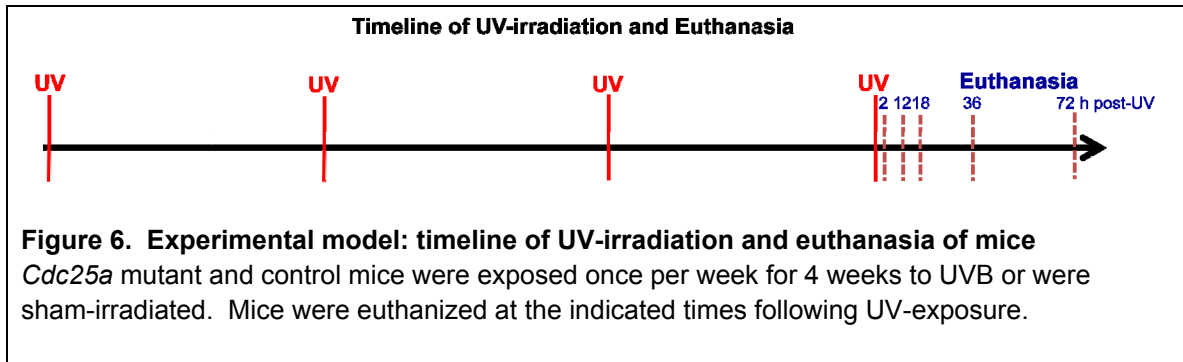
To test our hypothesis that ablation of CDC25A protein would result in decreased UV-induced skin tumorigenesis, skin-targeted *Cdc25a* mutant mice were developed (Figure 5A) using the Cre-LoxP system<sup>79</sup>. Skin-targeted *Cdc25a* knockout mice were obtained by breeding mice homozygous for loxP sites inserted flanking exons 1 through 3 of *Cdc25a* (*Cdc25a*<sup>fl/fl</sup>) with *Krt14* promoter-driven *Cre recombinase* (*Cre*<sup>+</sup>) mice (Figure 5A). Offspring were cross bred to generate skin-targeted *Cdc25a* knockout (*Cdc25a*<sup>fl/fl</sup>/*Cre*<sup>+</sup>) and control mice lacking *Cre* expression. *Cdc25a* mutant mice were healthy and viable, with no obvious gross phenotype. Immunoblotting using epidermal protein revealed reduced CDC25A protein in mutant epidermis (Figure 5B). Quantification of CDC25A in multiple immunoblots revealed a 60% decrease in CDC25A protein in mutant compared to control epidermis (Figure 5C). Thus, CDC25A was significantly reduced in the epidermis of the skin-targeted knockout mice.



*recombinase* driven by the Keratin 14 promoter. B. Immunoblot showing decreased levels of CDC25A in epidermis. C. Quantification of CDC25A levels as determined by immunoblot show a 60% decrease in CDC25A in *Cdc25a* mutant epidermis.

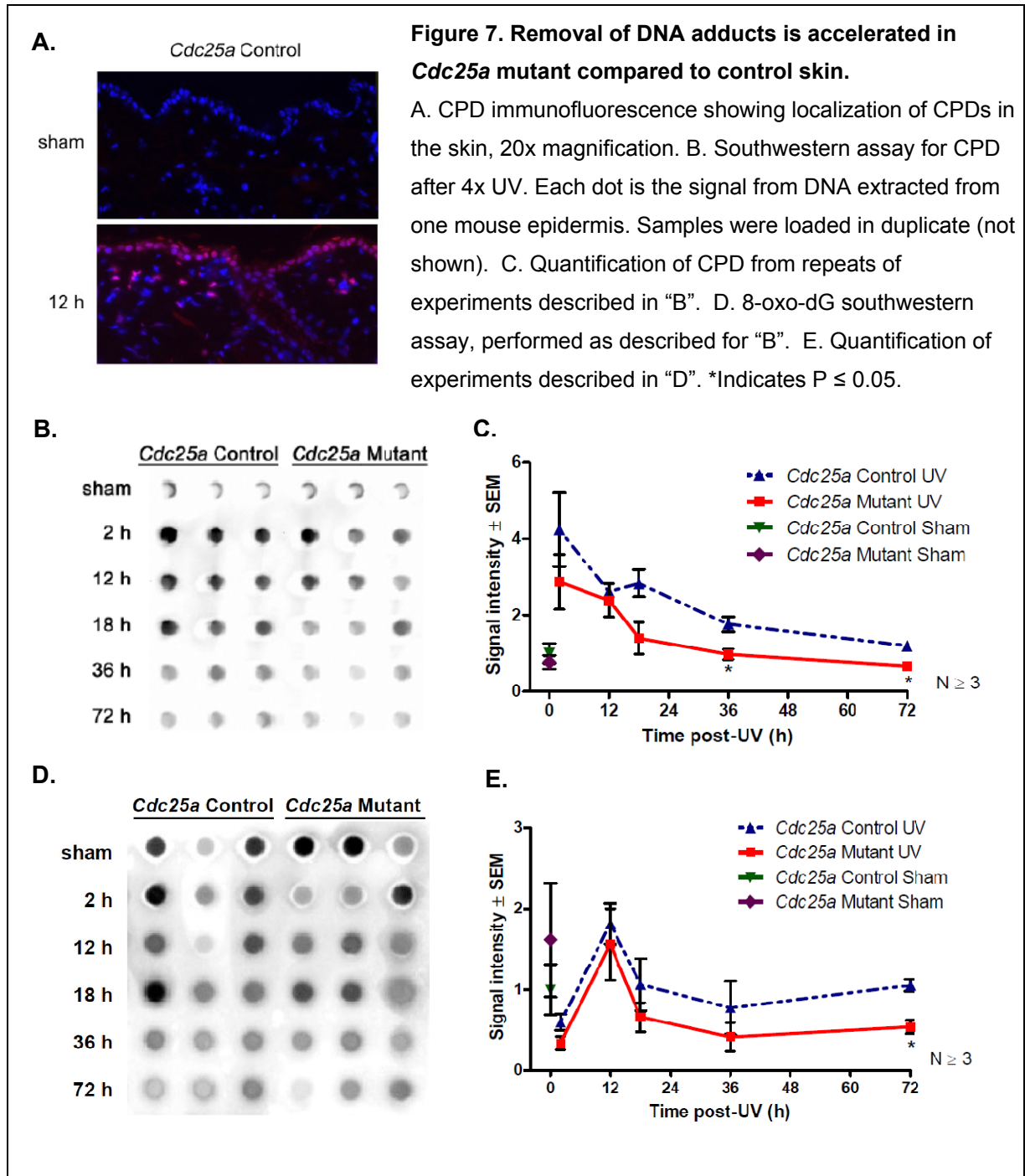
### ***Elimination of DNA damage was accelerated in UV-exposed Cdc25a mutant skin***

To prevent mutagenesis after DNA damage, the cell must have the ability to arrest cell cycle progression, allowing time for DNA repair before replication. To address the question of whether deletion of the CDK2 activator, CDC25A, allows for more efficient repair of DNA damage following UV-irradiation, groups of *Cdc25a* control and mutant mice were exposed to UV once a week for four weeks and euthanized at multiple time points after the final exposure according to the scheme shown in Figure 6.



UV-induced DNA damage in the form of cyclopurimidine dimers (CPDs) was detected using an antibody recognizing CPDs in DNA using a Southwestern blot assay and by immunofluorescence to examine localization of CPDs. As expected, CPDs were not detected by immunofluorescence of sham-irradiated *Cdc25a* control and mutant epidermis (Figure 7A, top panel). Following UV, CPD immunofluorescence was detected in both the epidermis and dermis between 2 h and 36 h (Figure 7A, bottom panel), and immunofluorescence was almost completely gone by 72 h following UV. In order to quantify the relative levels of CPDs present in *Cdc25a* control and mutant

epidermis following UV, a Southwestern assay was performed with isolated epidermis. Levels of cyclopuridine dimers peaked 2 h following UV in all mice, corresponding to the rapid formation of cyclopuridine dimers in both mutant and control mouse skin (Figure 7B and C). Levels of cyclopuridine dimers decreased after 2 h following UV exposure+. Consistent with our hypothesis, mutant *Cdc25a* skin eliminated cyclopuridine dimers from the epidermis more rapidly. Mutants had completely removed all UV-induced cyclopuridine dimers by 36 h following UV, whereas controls had still not completely eliminated them by 72 h (Figure 7C).



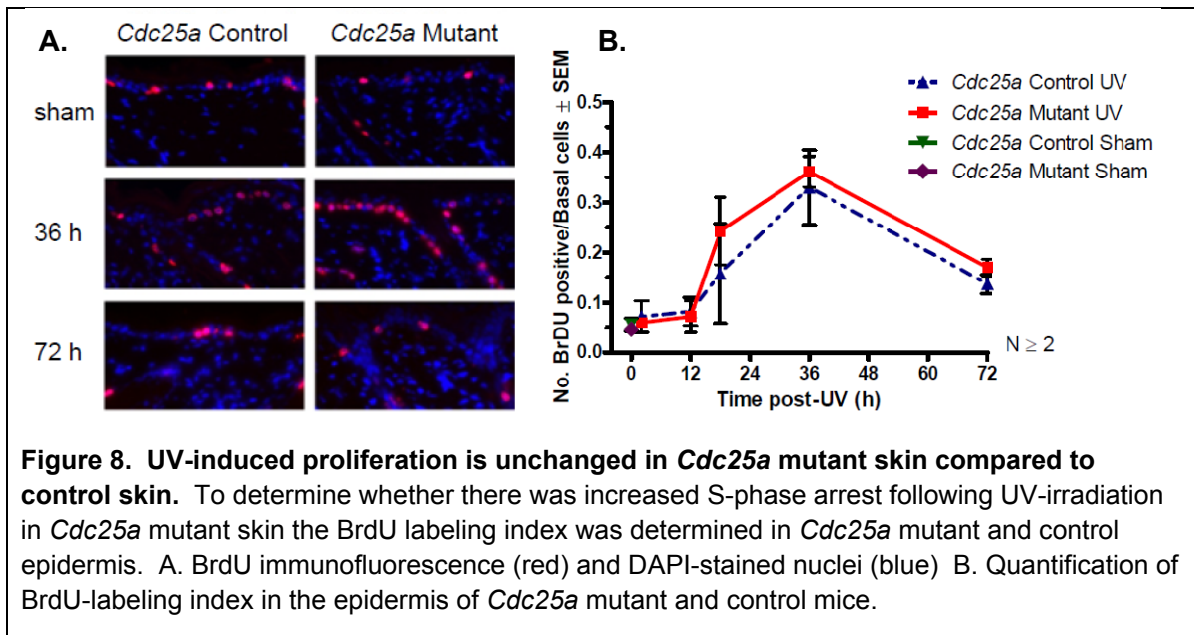
Another form of DNA damage resulting primarily from the formation of reactive oxygen species in response to UV irradiation is the 8-oxo-dG adduct. Southwestern assay was performed using an 8-oxo-dG antibody in order to quantify relative levels of 8-

oxo-dG in *Cdc25a* control and mutant epidermis. Surprisingly, sham-irradiated mouse skin had more 8-oxo-dG than at 2 h after UV for both *Cdc25a* controls and mutants (Figure 7D and E). Interestingly, Thomas-Ahner and colleagues observed significantly increased levels of 8-oxo-dG adducts in unirradiated male mouse skin compared to female mouse skin<sup>80</sup>, although we observed no gender-based differences in 8-oxo-dG levels in our assay. Thereafter, levels peaked at 12 h before declining. The 8-oxo-dG adducts were removed from *Cdc25a* mutant epidermis earlier than in controls, with significantly less in mutants compared to controls at 72 h following UV (Figure 7E). Consistent with our hypothesis, CPDs and 8-oxo-dG adducts were removed from *Cdc25a* mutant skin more quickly than in controls. These results suggest that ablation of *Cdc25a* in the skin allows for improved repair of UV-induced DNA damage in the skin.

#### ***S-phase and G<sub>2</sub>/M cells were increased in UV-irradiated Cdc25a mutant skin***

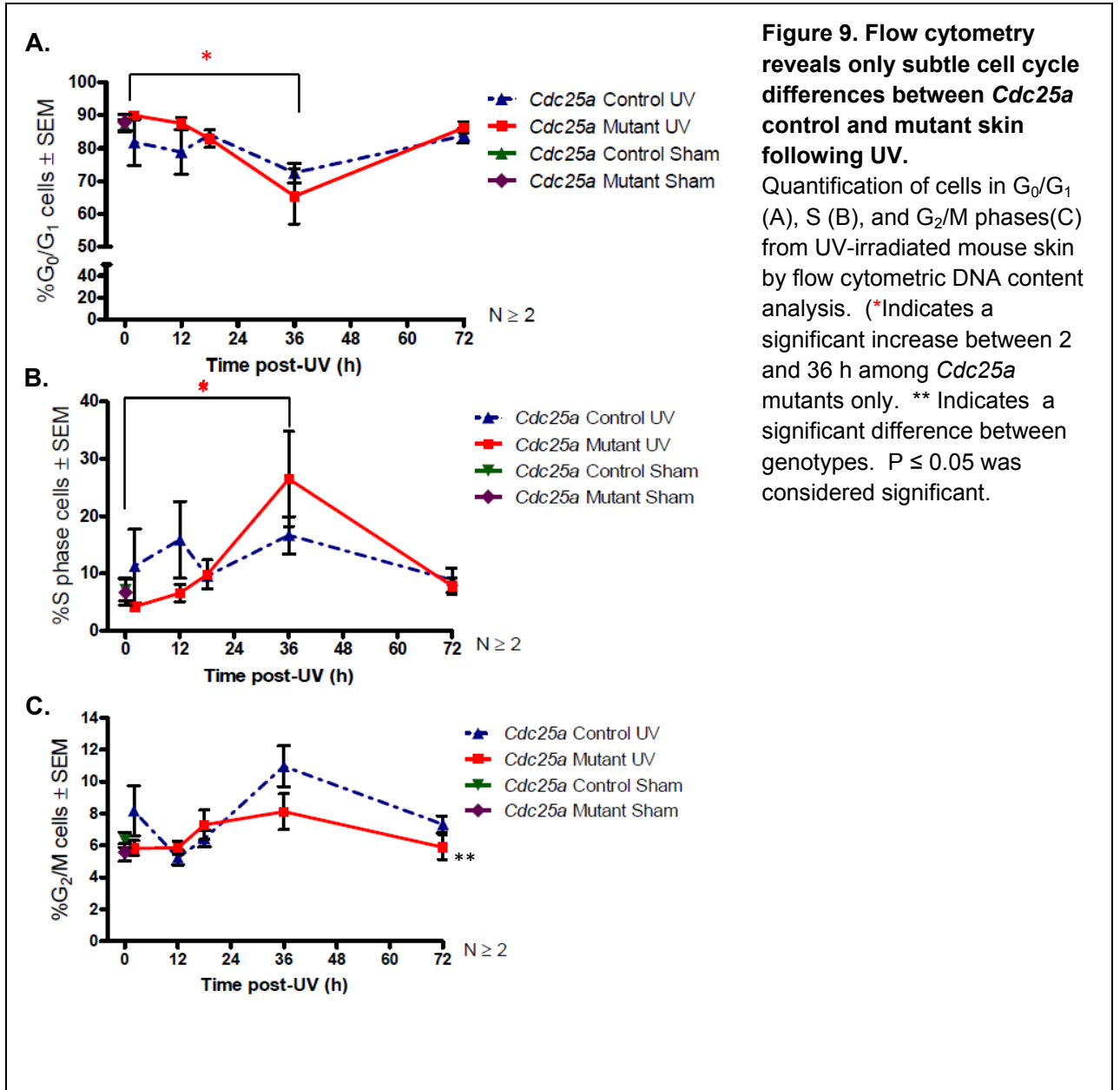
In order to determine whether improved repair of UV-induced DNA damage upon deletion of *Cdc25a* was due to greater cell cycle arrest, cell cycle analysis and cell proliferation were examined. Quantification of BrdU-positive cells as a measure of cell proliferation revealed no difference in the number of BrdU-positive cells in sham-irradiated *Cdc25a* mutant and control skin (Figure 8A). In contrast to our expectations, BrdU labeling was not significantly decreased in the first hours after UV-irradiation, which would have indicated a cell cycle arrest. There was little change in BrdU labeling after UV irradiation in both genotypes until 18 h (Figure 8B). By 18 h following UV, proliferation began to increase and then peaked at 36 h post-UV in both genotypes (Figure 8A,B). The BrdU labeling index decreased by 72 h post-UV but was still elevated when compared to sham-irradiated skin (Figure 8B). Surprisingly, there was no

significant difference in BrdU incorporation between the *Cdc25a* mutants and controls at any time point following UV irradiation.



To further examine the effect of CDC25A on the cell cycle, DNA content flow cytometry was performed. Similar to the BrdU incorporation results (Figure 8), the percentage of cells in S-phase increased between 2 h and 36 h post-UV for *Cdc25a* mutants ( $P=0.01$ ), consistent with increased proliferation during this time period, and then declined (Figure 9B).  $G_0/G_1$ -phase cells were decreased by a corresponding amount. Unlike controls, a decrease in the number of  $G_0/G_1$  cells between 2 h and 36 h post-UV was significant in *Cdc25a* mutant skin only ( $P=0.01$ ) (Figure 9A). In contrast to the mutants, S-phase cells were not significantly increased in *Cdc25a* control skin between 2 h and 36 h ( $P=0.60$ ) (Figure 9B). However, there was a second, earlier peak in S-phase cells at 12 h post-UV in *Cdc25a* control skin. Consistent with the BrdU incorporation data, no significant difference in the number of cells in S-phase was detected at any specific time point between the two genotypes (Figure 8, 9B), although S-phase

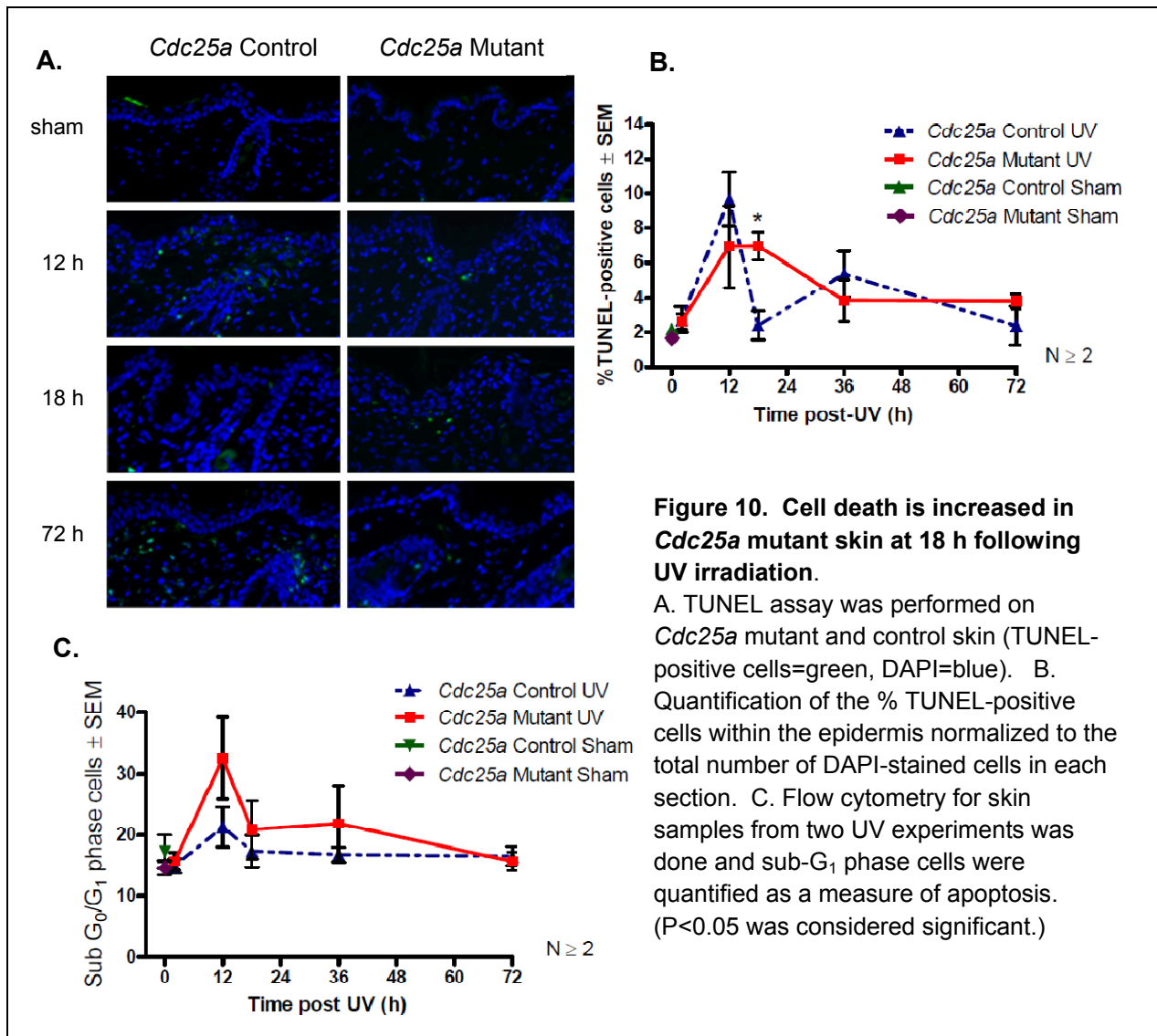
accumulation was significantly increased only in *Cdc25a* mutant skin between 2 and 36 h after UV exposure ( $P=0.01$ ) (Figure 9B). Interestingly, mean  $G_2/M$  phase cells were significantly reduced in UV-exposed *Cdc25a* mutant compared to control mice.(Figure 9C). Taken together, these results reveal only subtle effects of ablation of *Cdc25a* on proliferation or cell cycle control after UVR exposure.



### ***Apoptosis was increased in Cdc25a mutants following UV exposure***

Given that elimination of DNA damage was improved in the absence of increased cell cycle arrest in *Cdc25a* mutant skin, we further hypothesized that ablation of *Cdc25a* increased apoptosis in UV-irradiated skin. To examine apoptosis, both TUNEL and flow cytometry assays were used. The number of TUNEL-positive cells increased in both genotypes following UV exposure, peaking at 12 h and then decreasing to levels near baseline by 72 h (Figure 10A, B). Consistent with our hypothesis, *Cdc25a* mutant skin had significantly more TUNEL-positive cells at 18 hours following UV in comparison to control skin (Figure 10B). Analysis of sub-G<sub>0</sub>/G<sub>1</sub> cells using a DNA content flow cytometry assay revealed increased apoptosis in *Cdc25a* mutant skin at 12 h post-UV, while there was no significant increase in sub-G<sub>0</sub>/G<sub>1</sub> cells in the controls at this or any other time point (Figure 10C). Although the mean percentage of sub-G<sub>0</sub>/G<sub>1</sub> cells was higher in the *Cdc25a* mutants between 12 and 36 h post-UV, a direct comparison between the two genotypes revealed no statistically significant differences (P=0.09) (Figure 10C). Taken together, these results demonstrate that ablation of CDC25A in murine epidermis led to slightly increased apoptotic cell death following UV-irradiation.

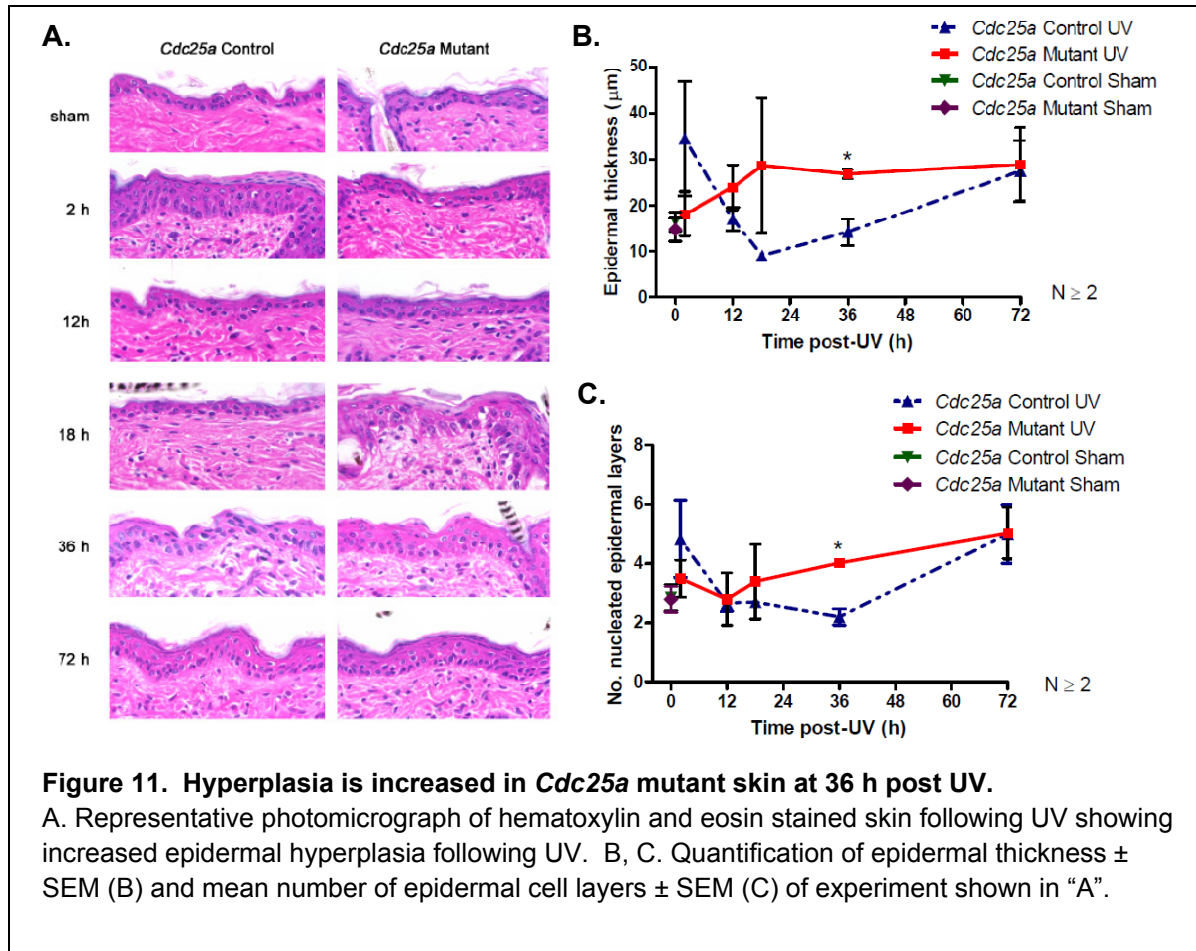




### *Ablation of Cdc25a altered the kinetics of epidermal hyperplasia following UV*

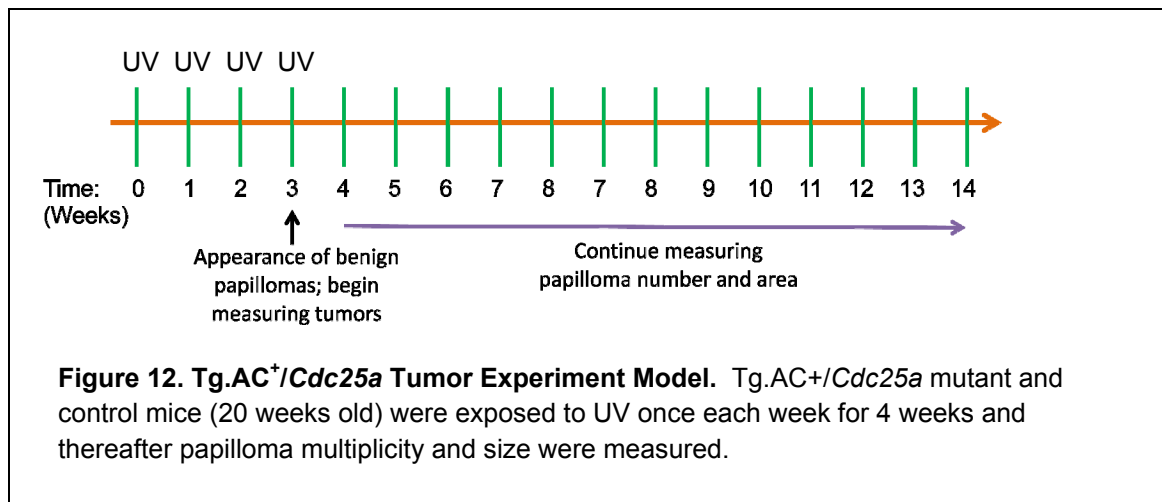
The hyperplastic response of the skin is a good predictor of the tumorigenic response in mouse skin<sup>81</sup>. Repeated exposure to UV induces epidermal hyperplasia<sup>82</sup>, which can be quantified by counting the number of nucleated epidermal cell layers and measuring epidermal thickness. Because of increased apoptosis in *Cdc25a* mutant skin after UV, we expected that *Cdc25a* mutants would have decreased epidermal hyperplasia following UV. Sham-irradiated *Cdc25a* mutant skin appeared histologically normal

(Figure 11A) and showed no differences in epidermal thickness or in the number of epidermal cell layers (Figure 11B,C). At 2 h post-UV, there was no difference in hyperplasia as compared to the sham-irradiated mice (Figure 11B, C). Thereafter, at 12 and 18 h post-UV, there was a slight decrease in nucleated cell layers, with no differences between genotypes at these times, followed by an increase between 18 and 72 h for both genotypes. By 36 h following UV, there was significantly more epidermal hyperplasia in the mutant epidermis compared to controls ( $P=0.03$ ), consistent with the increased percentage of S-phase cells in the flow cytometry experiment at 36 h (Figure 9B). By 72 h, both genotypes were similarly hyperplastic. These results suggest that ablation of *Cdc25a* leads to an increased hyperplastic response following UV irradiation.

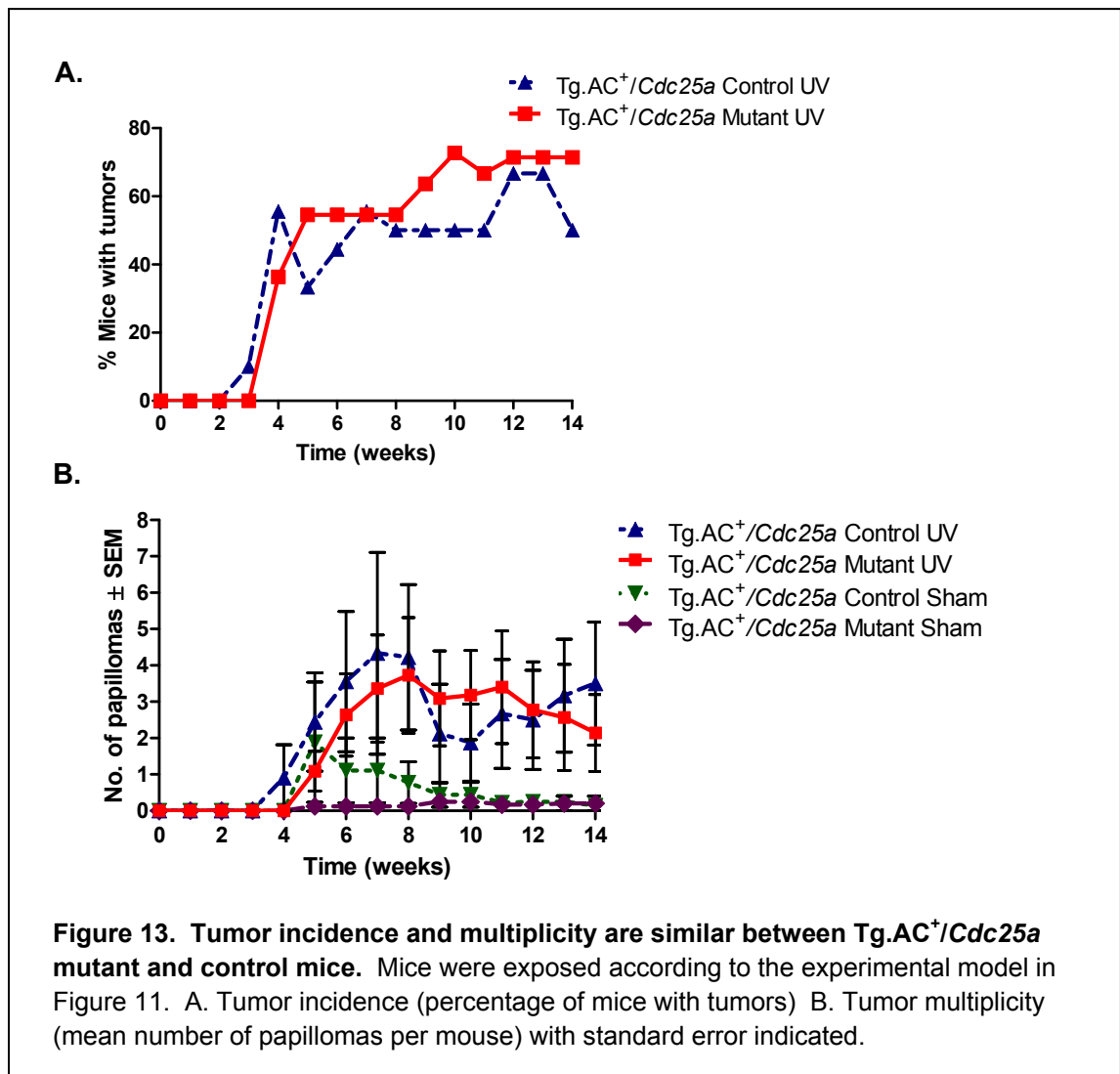


***Deletion of CDC25A did not alter the number of UV-induced tumors, but did increase tumor growth***

In order to examine the influence of CDC25A on UV-induced skin tumorigenesis, *Cdc25a* mutants and controls were crossed with *v-ras*<sup>Ha</sup> transgenic Tg.AC<sup>+</sup> mice, which are genetically initiated to develop skin papillomas after minimal exposure to UV<sup>83,84</sup>. These transgenic mice have markedly increased susceptibility to the development of UV-induced skin tumors. We exposed 20 week old *Cdc25a* control and mutant Tg.AC<sup>+</sup> mice to UV in order to determine whether there was a difference in the tumorigenic response (Figure 12).



Tumors were first observed in UV-exposed *Cdc25a* control mice at 3 weeks after the start of UV irradiation and at 4 weeks in the mutants (Figure 13A, B). By 5 weeks, *Tg.AC<sup>+</sup>/Cdc25a* mutants had an average of 1 tumor per mouse and controls had about 2.5 tumors per mouse. Tumor number in the controls peaked at with a mean of 4.3 tumors per mouse at 7 weeks. In the mutants, tumor number peaked at 8 weeks with nearly 4 tumors per mouse (Figure 13). Tumor multiplicity decreased after this due to euthanasia of moribund mice. There were no statistical differences in tumor multiplicity between genotypes at any time point.



Tumor area was measured weekly during the experiment (Figure 14D). Mean tumor area (Figure 14D) was calculated as the average area among all tumors within the group (and some mice in each group did not develop tumors), while mean tumor burden was calculated as the average tumor area per mouse for all mice in each group. Thus, mean tumor burden was a tumor area measurement which accounted for all of the mice in each group (Figure 14B).

Between 4 and 6 weeks following the start of the experiment, *Cdc25a* mutants had significantly decreased mean tumor area as compared to controls (Figure 14D). However, between 7 and 9 weeks post-UV there was a dramatic decrease in the mean

tumor area for the *Cdc25a* control group due to the euthanasia of one mouse with high tumor burden (Figure 14B, D). By 9 weeks, this trend was reversed and significantly larger tumors were present in the *Cdc25a* mutant group than in controls (Figure 14B, C, D). By 10 weeks, tumor areas were again similar in the two genotypes, as some mice in the UV-exposed mutant group were euthanized for health reasons, and tumor area did not significantly differ between the two groups for the duration of the experiment. To ensure that differences in tumor area were an effect of differences in CDC25A, levels of CDC25A, B, and C are currently being measured in papillomas from mice of both genotypes.

To determine whether ablation of CDC25A in the epidermis had an effect on the UV-induced inflammatory response in these Tg.AC<sup>+</sup> mice, which can aide in the development of skin tumors, skin-fold thickness measurements were taken each day for one week following the first UV exposure (data not shown)<sup>85</sup>. No differences in skin-fold thickness were observed between genotypes during this time frame, which suggested that ablation of *Cdc25a* had no effect on UV-induced edema.

Upon euthanasia, tumors were prepared for histopathological characterization using hematoxylin and eosin stained slides. Most of the lesions were squamous papillomas with a single squamous cell carcinoma in situ identified in each of the UV-exposed *Cdc25a* mutant and control groups. The squamous papillomas were well-circumscribed, exophytic tumors with marked papillomatosis, acanthosis, and variable hyperkeratosis (Figure 14C). Mitotic activity was minimal and no epithelial atypia or invasion was noted. In contrast, although the in situ squamous cell carcinomas showed similar configuration, increased mitotic activity and squamous atypia compared to

papillomas was observed, particularly among the basal cell layers of these tumors. While prominent epidermal “tongues” were observed originating from the basal epidermis, no frank invasion with surrounding desmoplasia was seen.

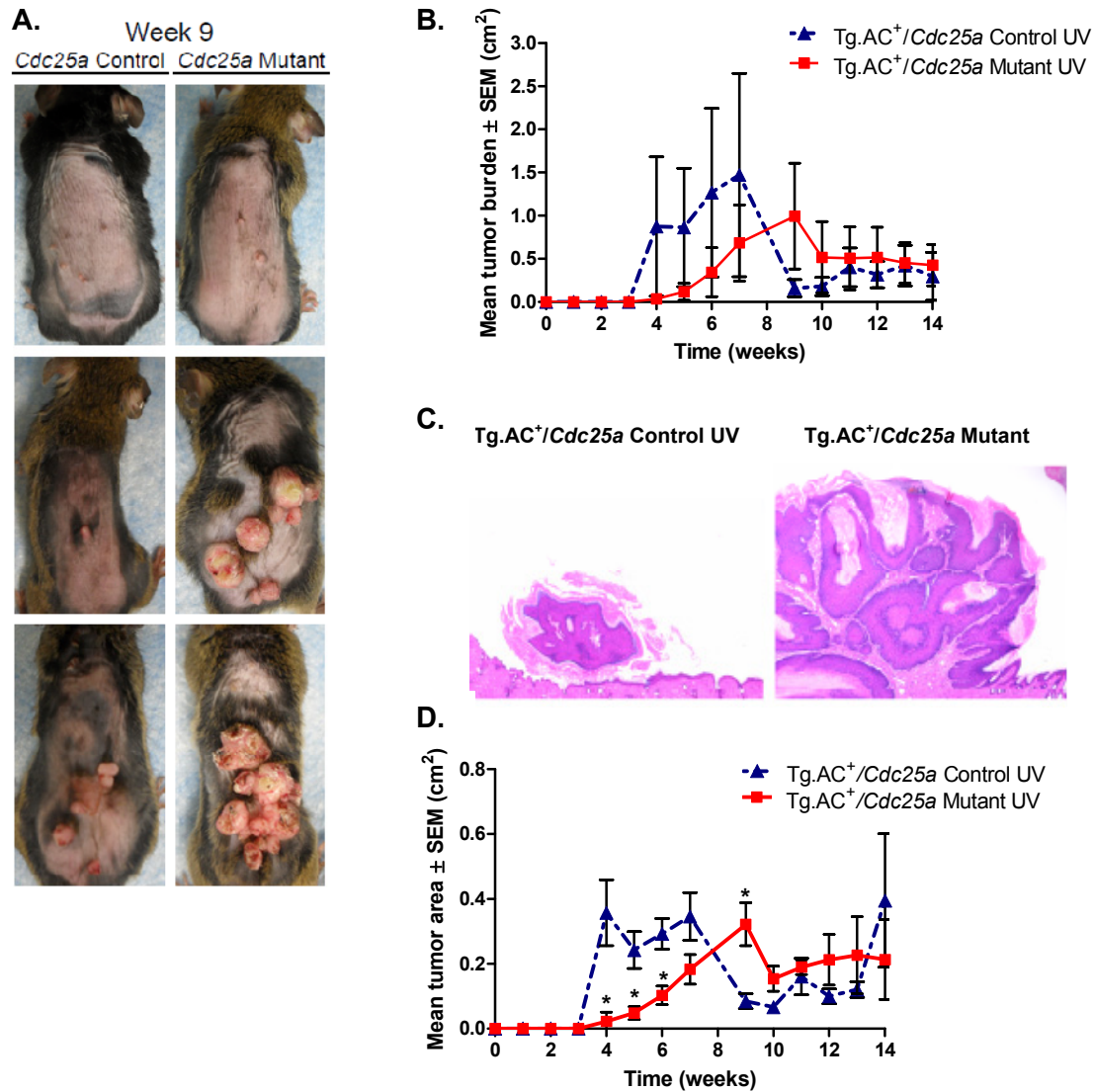


**Figure 14. UV-induced tumor development is altered in Tg.AC<sup>+</sup>/*Cdc25a* mutant compared to control mice** Tg.AC<sup>+</sup>/*Cdc25a* mutant and control mice were exposed to UV and tumor area was measured weekly after the development of benign papillomas. A. Representative photos of UV-irradiated mice at 9 weeks following the start of the experiment. B. Mean tumor burden for UV-irradiated mice with standard error marks (mean tumor area among all living mice for each group/timepoint). C. Photomicrographs of H&E stained papillomas from 9 week old *Cdc25a* mutant and control mice. D. Mean area among all tumors for each group. At weeks 4 through 6 *Cdc25a* mutants had significantly lower mean tumor area compared to controls. At week 9, however, mutants had significantly higher mean tumor area when compared to controls.



## Chapter 4: Discussion

The CDC25A phosphatase plays an important role in cell cycle regulation through its deactivation of cyclin-dependent kinases. Previous experiments in our laboratory have shown that in response to UV-irradiation, the receptor tyrosine kinase Erbb2 is activated and as a result keratinocytes progress through the S-phase of the cell cycle, which we hypothesized prevents efficient repair of DNA damage<sup>45</sup>. Ablation of Erbb2 leads to decreased levels of CDC25A as well as increased S-phase arrest following UV-irradiation. Because of these results, the role of CDC25A in UV-induced skin carcinogenesis and in the response of the skin to UV was investigated.

While CDC25A is over-expressed in a number of internal cancers including breast, colorectal, and esophageal cancer where it is associated with a poor prognosis<sup>64</sup>, little is known about the role of CDC25A in skin carcinogenesis. In order to investigate the role of CDC25A in non-melanoma skin tumorigenesis, a skin-targeted *Cdc25a* mutant mouse was created by utilizing a *Krt14* promoter-driven *Cre recombinase* gene. *Krt14* is expressed in the basal layer of the epidermis by embryonic day 14<sup>86</sup>, before development of hair follicles as outgrowths of the basal cells or differentiation of the basal layer into multilayered squamous epidermis<sup>87-89</sup>. We expected that *Cdc25a* would be targeted in all keratinocytes of the skin, both in the epidermis and the dermis. Our results are consistent with mosaicism of the cre/loxP system<sup>90</sup>, as our immunoblotting experiments revealed only a 60% decrease in CDC25A protein in *Cdc25a<sup>fl/fl</sup>/Cre<sup>+</sup>* epidermis.

This skin-targeted *Cdc25a* knockout model was used to investigate the hypothesis that deletion of *Cdc25a* increases cell cycle arrest following UV irradiation, resulting in improved repair of DNA damage and decreased skin tumorigenesis. Consistent with our

hypothesis which predicted that ablation of *Cdc25a* would lead to accelerated repair of UV-induced DNA damage through increased cell cycle arrest, the UV signature CPD lesion and the oxidized base, 8-oxo-dG were removed from the skin more rapidly in UV-exposed *Cdc25a* mutants when compared to UV-exposed control epidermis. However, the removal of DNA damaged lesions may have been due either to accelerated repair of the lesions or accelerated apoptosis of the DNA damaged cells. Because these lesions are repaired through distinct mechanisms, NER for CPDs and BER for 8-oxo-dG<sup>29</sup>, these results are consistent with CDC25A modulation of cell cycle arrest or cell death to facilitate elimination of the damage rather than a direct effect on DNA damage itself. Consequently, we anticipated that ablation of *Cdc25a* would increase S-phase arrest due to its established role in cell cycle regulation. Surprisingly, however, our assays revealed no cell cycle arrest after UV irradiation in mice of either genotype, but rather found increased proliferation beginning 18 h post-UV. Additionally, deletion of *Cdc25a* had only minor effects on the cell cycle after UV irradiation, including a statistical increase in the S-phase population of cells between 2 and 36 hours post-UV in mutant but not control skin and decreased G<sub>2</sub>/M-phase cells in *Cdc25a* mutant compared to control skin. This decrease in G<sub>2</sub>/M cells may be associated with decreased activation of cyclin B/CDK1 complex in the absence of CDC25A and consequent decreased entry into G<sub>2</sub>/M<sup>91</sup>, although this hypothesis remains uninvestigated. Thus, there appeared to be no cell cycle arrest with ablation of *Cdc25a*, although there were subtle differences in cell cycle regulation.

In the absence of cell cycle changes to account for improved elimination of UV-induced DNA damage, apoptotic cell death was examined. Apoptosis was increased in

the mutant skin compared to control at 18 hours following UV in a TUNEL assay. Similarly, sub-G<sub>0</sub>/G<sub>1</sub> cells were increased in mutant but not control cells after UV irradiation. Thus, accelerated removal of CPDs and 8-oxo-dG adducts in *Cdc25a* mutants is likely due to increased apoptosis of damaged cells in the absence of CDC25A. Experiments are underway to confirm this hypothesis using immunofluorescence to examine whether CPD-positive cells undergo apoptosis in *Cdc25a* mutant skin. A role of CDC25A in suppression of apoptotic cell death has previously been documented by Zou, et al. who found that CDC25A interacts directly with and inhibits apoptosis signal-regulating kinase 1 (ASK1), which is activated in response to reactive oxygen species and regulates multiple proteins involved in the cellular stress response pathway, such as the stress-activated protein kinases (SAPKs) and the p38 mitogen-activated protein kinase (MAPK)<sup>69</sup>. The stress response pathway leads to apoptosis. Thus, CDC25A may inhibit the apoptotic response to oxidative stress.

Changes in the cell cycle and apoptosis lead to altered epidermal hyperplasia, which results from the sum of changes in cell death and cell proliferation and is a robust and sensitive predictor of tumorigenic response in mouse skin models<sup>92</sup>. The kinetics of hyperplasia development in *Cdc25a* mutant skin appeared somewhat altered, with increased hyperplasia at 36 h post-UV compared to *Cdc25a* control skin. This is surprising given the increased cell death in *Cdc25a* mutant skin and in vitro experiments showing decreased proliferation with siRNA interference of *Cdc25a* expression<sup>93</sup>. This might be the result of altered timing of apoptotic cell death, which we observed as maintenance of peak levels of apoptotic cells at 18 hours following UV irradiation in *Cdc25a* mutant compared to control mice, and subtle alterations in cell cycle control in

the absence of CDC25A following UV-irradiation observed through cell cycle analysis by flow cytometry. The trend of increased numbers of BrdU-positive cells in *Cdc25a* mutants, although not statistically significant, suggests slightly increased proliferation in *Cdc25a* mutant epidermis compared to controls. This subtle difference in proliferation may have accumulated to produce changes in hyperplasia. The increased hyperplasia in *Cdc25a* mutant skin predicts that ablation of *Cdc25a* would lead to increased tumorigenesis, in contrast to our original hypothesis.

The influence of CDC25A on UV-induced tumor development was evaluated in  $\nu$ -ras<sup>Ha</sup> Tg.AC mice. There was no difference in tumor number or tumor initiation between *Cdc25a* mutant and control genotypes, which is less surprising due to the nature of the Tg.AC model, which appears to be genetically initiated to develop skin tumors. However, *Cdc25a* mutant mice were slower to develop skin tumors, as tumor area in the mutant group was statistically decreased compared to controls between weeks 4 and 6. This difference disappeared at later time points, as some mice with high tumor burdens were euthanized for humane reasons. Thus, in these experiments, ablation of *Cdc25a* did reduced tumor growth only early on but did not affect tumor number. These results are somewhat paradoxical given the improved elimination of DNA damage in the *Cdc25a* mutant mice, which predicts decreased tumorigenesis in the mutants. The lack of decrease in tumor number upon deletion of *Cdc25a* may be a consequence of the Tg.AC model used, since in this model tumor development correlates strongly with the proliferative and hyperplastic responses. Since only 4 exposures to UV are adequate to promote tumors in this model, UV-induced DNA damage may have less influence on tumorigenesis than UV-induced cell proliferation. An alternative to the Tg.AC model

would be the UV-irradiation of *Cdc25a*<sup>fl/fl</sup>/*Cre*<sup>+</sup> and *Cdc25a*<sup>fl/fl</sup>/*Cre*<sup>-</sup> mice on the hairless non-transgenic SKH-1 background, which requires up to 20 weeks of multi-week UV-irradiations for tumors to develop. Moreover, the Cre-LoxP system utilized produced an incomplete knockout of *Cdc25a* in the epidermis, since there was still 40% expression of *Cdc25a* in the epidermis. Thus it is possible that different results would be obtained with complete knockout of *Cdc25a*. Further analysis of CDC25A expression and localization in *Cdc25a* mutant epidermis are currently underway using Real Time PCR as well as immunohistochemistry. Alternatively, CDC25B and CDC25C may have compensated for the loss of CDC25A in the skin, since it has been shown that CDC25B and CDC25C have the ability to compensate for CDC25A in adult mice<sup>75</sup>. Several studies have been done which suggest a role for CDC25B and CDC25C in S-phase entry and progression<sup>94,95</sup>, although definitive modes of action are not known for mouse and human cells. Experiments are underway to assess the role of CDC25B and CDC25C in our experiments. By ablating these genes in combination as well as alone, information could be obtained about whether or not compensation by family members occurs.

To summarize, decreased levels of CDC25A in UV-irradiated skin resulted in accelerated removal of DNA damage in the epidermis and increased apoptotic cell death, which were accompanied by decreased tumor growth but no change in tumor number. Inhibitors of CDC25A have been developed such as the Vitamin K dual-specificity phosphatase inhibitor Cpd5, and the CDC25A-specific phenyl maleimide 20 (PM-20)<sup>96,97</sup>. PM-20 has been shown to reduce the tumor burden in rat liver cancer in vivo<sup>97</sup>. Thus, in other organs CDC25A has been shown to be a promising target for anti-cancer therapy. The data presented here, however, document improved elimination of DNA

damage, increased UV-induced apoptosis, and delayed tumor growth in *Cdc25a* mutant skin, but no differences in the number of UV-induced skin tumors in *Cdc25a* mutant mice. However, further experiments are required to fully evaluate the influence of CDC25A and its potential importance as a therapeutic target in skin cancer.

## Reference List

1. Young, B.; Lowe, J. S.; Stevens, A.; Heath, J. W. *Wheaters Functional Histology*; 2006.
2. Sun, T. T.; Shih, C.; Green, H. Keratin cytoskeletons in epithelial cells of internal organs. *Proc. Natl. Acad. Sci. U. S. A* **1979**, 76 (6), 2813-2817.
3. Fuchs, E. Keratins and the skin. *Annu. Rev. Cell Dev. Biol.* **1995**, 11, 123-153.
4. CARRUTHERS, C.; Suntzeff, V. Biochemistry and physiology of epidermis. *Physiol Rev.* **1953**, 33 (2), 229-243.
5. Sharp, L. L.; Jameson, J. M.; Cauvi, G.; Havran, W. L. Dendritic epidermal T cells regulate skin homeostasis through local production of insulin-like growth factor 1. *Nat. Immunol.* **2005**, 6 (1), 73-79.
6. Maklad, A.; Nicolai, J. R.; Bichsel, K. J.; Evenson, J. E.; Lee, T. C.; Threadgill, D. W.; Hansen, L. A. The EGFR is required for proper innervation to the skin. *J. Invest Dermatol.* **2009**, 129 (3), 690-698.
7. Green, K. J.; Jones, J. C. Desmosomes and hemidesmosomes: structure and function of molecular components. *FASEB J.* **1996**, 10 (8), 871-881.
8. Humphries, M. J. Integrin cell adhesion receptors and the concept of agonism. *Trends Pharmacol. Sci.* **2000**, 21 (1), 29-32.
9. Peltonen, S.; Raiko, L.; Peltonen, J. Desmosomes in developing human epidermis. *Dermatol. Res. Pract.* **2010**, 2010, 698761.
10. Margolis, B.; Borg, J. P. Apicobasal polarity complexes. *J. Cell Sci.* **2005**, 118 (Pt 22), 5157-5159.

11. Perez-Moreno, M.; Jamora, C.; Fuchs, E. Sticky business: orchestrating cellular signals at adherens junctions. *Cell* **2003**, *112* (4), 535-548.
12. Becker, W. M.; Kleinsmith, L. J.; Hardin, J. *The World of the Cell*; 6 ed.; Pearson Education: San Francisco, 2006.
13. Garrod, D. R.; Merritt, A. J.; Nie, Z. Desmosomal adhesion: structural basis, molecular mechanism and regulation (Review). *Mol. Membr. Biol.* **2002**, *19* (2), 81-94.
14. Fuchs, E. Scratching the surface of skin development. *Nature* **2007**, *445* (7130), 834-842.
15. Koster, M. I.; Roop, D. R. Asymmetric cell division in skin development: a new look at an old observation. *Dev. Cell* **2005**, *9* (4), 444-446.
16. Lechler, T.; Fuchs, E. Asymmetric cell divisions promote stratification and differentiation of mammalian skin. *Nature* **2005**, *437* (7056), 275-280.
17. Bikle, D. D. Vitamin D and the skin. *J. Bone Miner. Metab* **2010**, *28* (2), 117-130.
18. Denning, M. F. Tightening the epidermal barrier with atypical PKCs. *J. Invest Dermatol.* **2007**, *127* (4), 742-744.
19. Chilcott, R.; Price, S. *Principles and Practice of Skin Toxicology*; Wiley: 2008.
20. Botchkarev, V. A.; Eichmuller, S.; Johansson, O.; Paus, R. Hair cycle-dependent plasticity of skin and hair follicle innervation in normal murine skin. *J. Comp Neurol.* **1997**, *386* (3), 379-395.
21. Braverman, I. M. Ultrastructure and organization of the cutaneous microvasculature in normal and pathologic states. *J. Invest Dermatol.* **1989**, *93* (2 Suppl), 2S-9S.



22. Hedrich, H. *The Laboratory Mouse*; Elsevier Limited: San Diego, 2004.
23. Trakatelli, M.; Ulrich, C.; Del, M., V; Euvrard, S.; Stockfleth, E.; Abeni, D.  
Epidemiology of nonmelanoma skin cancer (NMSC) in Europe: accurate and comparable data are needed for effective public health monitoring and interventions. *Br. J. Dermatol.* **2007**, *156 Suppl 3*, 1-7.
24. Rogers, H. W.; Weinstock, M. A.; Harris, A. R.; Hinckley, M. R.; Feldman, S. R.; Fleischer, A. B.; Coldiron, B. M. Incidence estimate of nonmelanoma skin cancer in the United States, 2006. *Arch. Dermatol.* **2010**, *146* (3), 283-287.
25. Strom, S. S.; Yamamura, Y. Epidemiology of nonmelanoma skin cancer. *Clin. Plast. Surg.* **1997**, *24* (4), 627-636.
26. Geller, A. C.; Annas, G. D. Epidemiology of melanoma and nonmelanoma skin cancer. *Semin. Oncol. Nurs.* **2003**, *19* (1), 2-11.
27. de Gruijl, F. R.; van Kranen, H. J.; Mullenders, L. H. UV-induced DNA damage, repair, mutations and oncogenic pathways in skin cancer. *J. Photochem. Photobiol. B* **2001**, *63* (1-3), 19-27.
28. Rass, K.; Reichrath, J. UV damage and DNA repair in malignant melanoma and nonmelanoma skin cancer. *Adv. Exp. Med. Biol.* **2008**, *624*, 162-178.
29. Marrot, L.; Meunier, J. R. Skin DNA photodamage and its biological consequences. *J. Am. Acad. Dermatol.* **2008**, *58* (5 Suppl 2), S139-S148.
30. Lo, H. L.; Nakajima, S.; Ma, L.; Walter, B.; Yasui, A.; Ethell, D. W.; Owen, L. B. Differential biologic effects of CPD and 6-4PP UV-induced DNA damage on the induction of apoptosis and cell-cycle arrest. *BMC. Cancer* **2005**, *5*, 135.

31. You, Y. H.; Lee, D. H.; Yoon, J. H.; Nakajima, S.; Yasui, A.; Pfeifer, G. P. Cyclobutane pyrimidine dimers are responsible for the vast majority of mutations induced by UVB irradiation in mammalian cells. *J. Biol. Chem.* **2001**, 276 (48), 44688-44694.
32. Strydom, A.; Robert, C.; Sarasin, A. Deleterious effects of ultraviolet A radiation in human cells. *Mutat. Res.* **1997**, 383 (1), 1-8.
33. Halliday, G. M. Inflammation, gene mutation and photoimmunosuppression in response to UVR-induced oxidative damage contributes to photocarcinogenesis. *Mutat. Res.* **2005**, 571 (1-2), 107-120.
34. Shigenaga, M. K.; Gimeno, C. J.; Ames, B. N. Urinary 8-hydroxy-2'-deoxyguanosine as a biological marker of in vivo oxidative DNA damage. *Proc. Natl. Acad. Sci. U. S. A* **1989**, 86 (24), 9697-9701.
35. Kasai, H.; Nishimura, S. Hydroxylation of deoxyguanosine at the C-8 position by ascorbic acid and other reducing agents. *Nucleic Acids Res.* **1984**, 12 (4), 2137-2145.
36. Sancar, A.; Lindsey-Boltz, L. A.; Unsal-Kacmaz, K.; Linn, S. Molecular mechanisms of mammalian DNA repair and the DNA damage checkpoints. *Annu. Rev. Biochem.* **2004**, 73, 39-85.
37. Abraham, R. T. Cell cycle checkpoint signaling through the ATM and ATR kinases. *Genes Dev.* **2001**, 15 (17), 2177-2196.
38. Namiki, Y.; Zou, L. ATRIP associates with replication protein A-coated ssDNA through multiple interactions. *Proc. Natl. Acad. Sci. U. S. A* **2006**, 103 (3), 580-585.

39. Zou, L.; Elledge, S. J. Sensing DNA damage through ATRIP recognition of RPA-ssDNA complexes. *Science* **2003**, *300* (5625), 1542-1548.
40. Unsal-Kacmaz, K.; Makhov, A. M.; Griffith, J. D.; Sancar, A. Preferential binding of ATR protein to UV-damaged DNA. *Proc. Natl. Acad. Sci. U. S. A* **2002**, *99* (10), 6673-6678.
41. Epstein, J. H.; Fukuyama, K.; Fye, K. Effects of ultraviolet radiation on the mitotic cycle and DNA, RNA and protein synthesis in mammalian epidermis in vivo. *Photochem. Photobiol.* **1970**, *12* (1), 57-65.
42. Pavey, S.; Russell, T.; Gabrielli, B. G2 phase cell cycle arrest in human skin following UV irradiation. *Oncogene* **2001**, *20* (43), 6103-6110.
43. Dunphy, W. G.; Kumagai, A. The cdc25 protein contains an intrinsic phosphatase activity. *Cell* **1991**, *67* (1), 189-196.
44. Huang, R. P.; Wu, J. X.; Fan, Y.; Adamson, E. D. UV activates growth factor receptors via reactive oxygen intermediates. *J. Cell Biol.* **1996**, *133* (1), 211-220.
45. Madson, J. G.; Lynch, D. T.; Svoboda, J.; Ophardt, R.; Yanagida, J.; Putta, S. K.; Bowles, A.; Trempus, C. S.; Tennant, R. W.; Hansen, L. A. Erbb2 suppresses DNA damage-induced checkpoint activation and UV-induced mouse skin tumorigenesis. *Am. J. Pathol.* **2009**, *174* (6), 2357-2366.
46. Shtivelman, E.; Sussman, J.; Stokoe, D. A role for PI 3-kinase and PKB activity in the G2/M phase of the cell cycle. *Curr. Biol.* **2002**, *12* (11), 919-924.
47. Brash, D. E.; Rudolph, J. A.; Simon, J. A.; Lin, A.; McKenna, G. J.; Baden, H. P.; Halperin, A. J.; Ponten, J. A role for sunlight in skin cancer: UV-induced

- p53 mutations in squamous cell carcinoma. *Proc. Natl. Acad. Sci. U. S. A* **1991**, 88 (22), 10124-10128.
48. Farage, M. A.; Miller, K. W.; Maibach, H. I. *Textbook of Aging Skin*; Springer: Berlin, 2010.
  49. Tornaletti, S.; Pfeifer, G. P. Slow repair of pyrimidine dimers at p53 mutation hotspots in skin cancer. *Science* **1994**, 263 (5152), 1436-1438.
  50. McGregor, W. G.; Chen, R. H.; Lukash, L.; Maher, V. M.; McCormick, J. J. Cell cycle-dependent strand bias for UV-induced mutations in the transcribed strand of excision repair-proficient human fibroblasts but not in repair-deficient cells. *Mol. Cell Biol.* **1991**, 11 (4), 1927-1934.
  51. Klein, J. C.; Bleeker, M. J.; Saris, C. P.; Roelen, H. C.; Brugghe, H. F.; van den Elst, H.; van der Marel, G. A.; van Boom, J. H.; Westra, J. G.; Kriek, E.; . Repair and replication of plasmids with site-specific 8-oxodG and 8-AAFdG residues in normal and repair-deficient human cells. *Nucleic Acids Res.* **1992**, 20 (17), 4437-4443.
  52. Kamiya, H.; Miura, K.; Ishikawa, H.; Inoue, H.; Nishimura, S.; Ohtsuka, E. c-Ha-ras containing 8-hydroxyguanine at codon 12 induces point mutations at the modified and adjacent positions. *Cancer Res.* **1992**, 52 (12), 3483-3485.
  53. van der Schroeff, J. G.; Evers, L. M.; Boot, A. J.; Bos, J. L. Ras oncogene mutations in basal cell carcinomas and squamous cell carcinomas of human skin. *J. Invest Dermatol.* **1990**, 94 (4), 423-425.

54. Pierceall, W. E.; Kripke, M. L.; Ananthaswamy, H. N. N-ras mutation in ultraviolet radiation-induced murine skin cancers. *Cancer Res.* **1992**, *52* (14), 3946-3951.
55. Ananthaswamy, H. N.; Pierceall, W. E. Molecular alterations in human skin tumors. *Prog. Clin. Biol. Res.* **1992**, *376*, 61-84.
56. Pierceall, W. E.; Goldberg, L. H.; Tainsky, M. A.; Mukhopadhyay, T.; Ananthaswamy, H. N. Ras gene mutation and amplification in human nonmelanoma skin cancers. *Mol. Carcinog.* **1991**, *4* (3), 196-202.
57. Ruddon, R. W. *Cancer Biology*; 3rd ed.; 1995.
58. Anderson, M. W.; Reynolds, S. H.; You, M.; Maronpot, R. M. Role of proto-oncogene activation in carcinogenesis. *Environ. Health Perspect.* **1992**, *98*, 13-24.
59. Hong, H. L.; Devereux, T. R.; Melnick, R. L.; Eldridge, S. R.; Greenwell, A.; Haseman, J.; Boorman, G. A.; Sills, R. C. Both K-ras and H-ras protooncogene mutations are associated with Harderian gland tumorigenesis in B6C3F1 mice exposed to isoprene for 26 weeks. *Carcinogenesis* **1997**, *18* (4), 783-789.
60. Chu, I. M.; Hengst, L.; Slingerland, J. M. The Cdk inhibitor p27 in human cancer: prognostic potential and relevance to anticancer therapy. *Nat. Rev. Cancer* **2008**, *8* (4), 253-267.
61. Cangi, M. G.; Piccinin, S.; Pecciarini, L.; Talarico, A.; Dal, C. E.; Grassi, S.; Grizzo, A.; Maestro, R.; Doglioni, C. Constitutive overexpression of CDC25A in primary human mammary epithelial cells results in both

defective DNA damage response and chromosomal breaks at fragile sites.

*Int. J. Cancer* **2008**, *123* (6), 1466-1471.

62. Xu, X.; Yamamoto, H.; Sakon, M.; Yasui, M.; Ngan, C. Y.; Fukunaga, H.; Morita, T.; Ogawa, M.; Nagano, H.; Nakamori, S.; Sekimoto, M.; Matsuura, N.; Monden, M. Overexpression of CDC25A phosphatase is associated with hypergrowth activity and poor prognosis of human hepatocellular carcinomas. *Clin. Cancer Res.* **2003**, *9* (5), 1764-1772.
63. Cho, H.; Krishnaraj, R.; Kitas, E.; Bannwarth, W.; Walsh, C. T.; Anderson, K. S. Isolation and structural elucidation of a novel phosphocysteine intermediate in the LAR protein tyrosine phosphatase enzymic pathway. *J. Am. Chem. Soc.* **1992**.
64. Boutros, R.; Lobjois, V.; Ducommun, B. CDC25 phosphatases in cancer cells: key players? Good targets? *Nat. Rev. Cancer* **2007**, *7* (7), 495-507.
65. Cangi, M. G.; Cukor, B.; Soung, P.; Signoretti, S.; Moreira, G., Jr.; Ranashinge, M.; Cady, B.; Pagano, M.; Loda, M. Role of the Cdc25A phosphatase in human breast cancer. *J. Clin. Invest* **2000**, *106* (6), 753-761.
66. Weinberg, R. A. *The Biology of Cancer*; 2007.
67. Kiyokawa, H.; Ray, D. In vivo roles of CDC25 phosphatases: biological insight into the anti-cancer therapeutic targets. *Anticancer Agents Med. Chem.* **2008**, *8* (8), 832-836.
68. Galaktionov, K.; Lee, A. K.; Eckstein, J.; Draetta, G.; Meckler, J.; Loda, M.; Beach, D. CDC25 phosphatases as potential human oncogenes. *Science* **1995**, *269* (5230), 1575-1577.

69. Zou, X.; Tsutsui, T.; Ray, D.; Blomquist, J. F.; Ichijo, H.; Ucker, D. S.; Kiyokawa, H. The cell cycle-regulatory CDC25A phosphatase inhibits apoptosis signal-regulating kinase 1. *Mol. Cell Biol.* **2001**, *21* (14), 4818-4828.
70. Matsukawa, J.; Matsuzawa, A.; Takeda, K.; Ichijo, H. The ASK1-MAP kinase cascades in mammalian stress response. *J. Biochem.* **2004**, *136* (3), 261-265.
71. Nishikawa, Y.; Carr, B. I.; Wang, M.; Kar, S.; Finn, F.; Dowd, P.; Zheng, Z. B.; Kerns, J.; Naganathan, S. Growth inhibition of hepatoma cells induced by vitamin K and its analogs. *J. Biol. Chem.* **1995**, *270* (47), 28304-28310.
72. Kar, S.; Adachi, T.; Carr, B. I. EGFR-independent activation of ERK1/2 mediates growth inhibition by a PTPase antagonizing K-vitamin analog. *J. Cell Physiol* **2002**, *190* (3), 356-364.
73. Kar, S.; Carr, B. I. Growth inhibition and protein tyrosine phosphorylation in MCF 7 breast cancer cells by a novel K vitamin. *J. Cell Physiol* **2000**, *185* (3), 386-393.
74. Kar, S.; Lefterov, I. M.; Wang, M.; Lazo, J. S.; Scott, C. N.; Wilcox, C. S.; Carr, B. I. Binding and inhibition of Cdc25 phosphatases by vitamin K analogues. *Biochemistry* **2003**, *42* (35), 10490-10497.
75. Lee, G.; White, L. S.; Hurov, K. E.; Stappenbeck, T. S.; Piwnicka-Worms, H. Response of small intestinal epithelial cells to acute disruption of cell division through CDC25 deletion. *Proc. Natl. Acad. Sci. U. S. A* **2009**, *106* (12), 4701-4706.

76. Hansen, L. A.; Monteiro-Riviere, N. A.; Smart, R. C. Differential down-regulation of epidermal protein kinase C by 12-O-tetradecanoylphorbol-13-acetate and diacylglycerol: association with epidermal hyperplasia and tumor promotion. *Cancer Res.* **1990**, *50* (18), 5740-5745.
77. Vindelov, L. L. Flow microfluorometric analysis of nuclear DNA in cells from solid tumors and cell suspensions. A new method for rapid isolation and straining of nuclei. *Virchows Arch. B Cell Pathol.* **1977**, *24* (3), 227-242.
78. Wulff, B. C.; Schick, J. S.; Thomas-Ahner, J. M.; Kusewitt, D. F.; Yarosh, D. B.; Oberszyn, T. M. Topical treatment with OGG1 enzyme affects UVB-induced skin carcinogenesis. *Photochem. Photobiol.* **2008**, *84* (2), 317-321.
79. Gu, H.; Marth, J. D.; Orban, P. C.; Mossmann, H.; Rajewsky, K. Deletion of a DNA polymerase beta gene segment in T cells using cell type-specific gene targeting. *Science* **1994**, *265* (5168), 103-106.
80. Thomas-Ahner, J. M.; Wulff, B. C.; Tober, K. L.; Kusewitt, D. F.; Riggensbach, J. A.; Oberszyn, T. M. Gender differences in UVB-induced skin carcinogenesis, inflammation, and DNA damage. *Cancer Res.* **2007**, *67* (7), 3468-3474.
81. Fuhrman, J.; Shafer, L.; Repertinger, S.; Chan, T.; Hansen, L. A. Mechanisms of SEPA 0009-induced tumorigenesis in v-rasHa transgenic Tg.AC mice. *Toxicol. Pathol.* **2005**, *33* (6), 623-630.
82. Maronpot, R. R. *Pathology of the Mouse*; Cache River Press: Vienna, 1999.pp. 555-570.



83. Leder, A.; Kuo, A.; Cardiff, R. D.; Sinn, E.; Leder, P. v-Ha-ras transgene abrogates the initiation step in mouse skin tumorigenesis: effects of phorbol esters and retinoic acid. *Proc. Natl. Acad. Sci. U. S. A* **1990**, *87* (23), 9178-9182.
84. Trempus, C. S.; Mahler, J. F.; Ananthaswamy, H. N.; Loughlin, S. M.; French, J. E.; Tennant, R. W. Photocarcinogenesis and susceptibility to UV radiation in the v-Ha-ras transgenic Tg.AC mouse. *J. Invest Dermatol.* **1998**, *111* (3), 445-451.
85. Tober, K. L.; Wilgus, T. A.; Kusewitt, D. F.; Thomas-Ahner, J. M.; Maruyama, T.; Oberyshyn, T. M. Importance of the EP(1) receptor in cutaneous UVB-induced inflammation and tumor development. *J. Invest Dermatol.* **2006**, *126* (1), 205-211.
86. Dassule, H. R.; Lewis, P.; Bei, M.; Maas, R.; McMahon, A. P. Sonic hedgehog regulates growth and morphogenesis of the tooth. *Development* **2000**, *127* (22), 4775-4785.
87. Lloyd, C.; Yu, Q. C.; Cheng, J.; Turksen, K.; Degenstein, L.; Hutton, E.; Fuchs, E. The basal keratin network of stratified squamous epithelia: defining K15 function in the absence of K14. *J. Cell Biol.* **1995**, *129* (5), 1329-1344.
88. Byrne, C.; Tainsky, M.; Fuchs, E. Programming gene expression in developing epidermis. *Development* **1994**, *120* (9), 2369-2383.
89. Yu, B. D.; Mukhopadhyay, A.; Wong, C. Skin and hair: models for exploring organ regeneration. *Hum. Mol. Genet.* **2008**, *17* (R1), R54-R59.

90. Nagy, A. Cre recombinase: the universal reagent for genome tailoring. *Genesis*. **2000**, 26 (2), 99-109.
91. Mailand, N.; Podtelejnikov, A. V.; Groth, A.; Mann, M.; Bartek, J.; Lukas, J.  
Regulation of G(2)/M events by Cdc25A through phosphorylation-dependent modulation of its stability. *EMBO J.* **2002**, 21 (21), 5911-5920.
92. Lynch, D.; Svoboda, J.; Putta, S.; Hofland, H. E.; Chern, W. H.; Hansen, L. A.  
Mouse skin models for carcinogenic hazard identification: utilities and challenges. *Toxicol. Pathol.* **2007**, 35 (7), 853-864.
93. Yamashita, Y.; Kasugai, I.; Sato, M.; Tanuma, N.; Sato, I.; Nomura, M.;  
Yamashita, K.; Sonoda, Y.; Kumabe, T.; Tominaga, T.; Katakura, R.;  
Shima, H. CDC25A mRNA levels significantly correlate with Ki-67  
expression in human glioma samples. *Journal of Neurooncology* **2010**, 99.
94. Garner-Hamrick, P. A.; Fisher, C. Antisense phosphorothioate oligonucleotides  
specifically down-regulate cdc25B causing S-phase delay and persistent  
antiproliferative effects. *Int. J. Cancer* **1998**, 76 (5), 720-728.
95. Turowski, P.; Franckhauser, C.; Morris, M. C.; Vaglio, P.; Fernandez, A.; Lamb,  
N. J. Functional cdc25C dual-specificity phosphatase is required for S-  
phase entry in human cells. *Mol. Biol. Cell* **2003**, 14 (7), 2984-2998.
96. Kar, S.; Wang, M.; Wilcox, C. S.; Carr, B. I. Antitumor and anticarcinogenic  
actions of Cpd 5: a new class of protein phosphatase inhibitor.  
*Carcinogenesis* **2003**, 24 (3), 411-416.
97. Kar, S.; Wang, M.; Yao, W.; Michejda, C. J.; Carr, B. I. PM-20, a novel inhibitor  
of Cdc25A, induces extracellular signal-regulated kinase 1/2

phosphorylation and inhibits hepatocellular carcinoma growth in vitro and in vivo. *Mol. Cancer Ther.* **2006**, 5 (6), 1511-1519.